

- biotherapy: a novel therapeutic platform. *Lancet Oncol* 2002;3:17–26.
8. Kawashima T, Kagawa S, Kobayashi N, et al. Telomerase-specific replication-selective virotherapy for human cancer. *Clin Cancer Res* 2004;10:285–92.
 9. Taki M, Kagawa S, Nishizaki M, et al. Enhanced oncolysis by a tropism-modified telomerase-specific replication-selective adenoviral agent OBP-405 ('Telomelysin-RGD'). *Oncogene* 2005;24:3130–40.
 10. Hashimoto Y, Watanabe Y, Shirakiya Y, et al. Establishment of biological and pharmacokinetic assays of telomerase-specific replication-selective adenovirus. *Cancer Sci* 2008;99:385–90.
 11. Kishimoto H, Kojima T, Watanabe Y, et al. *In vivo* imaging of lymph node metastasis with telomerase-specific replication-selective adenovirus. *Nat Med* 2006;12:1213–9.
 12. Kotwall C, Sako K, Razack MS, Rao U, Bakamjian V, Shedd DP. Metastatic patterns in squamous cell cancer of the head and neck. *Am J Surg* 1987;154:439–42.
 13. Myers JN, Holsinger FC, Jasser SA, Bekele BN, Fidler IJ. An orthotopic nude mouse model of oral tongue squamous cell carcinoma. *Clin Cancer Res* 2002;8:293–8.
 14. Fujiwara T, Kagawa S, Kishimoto H, et al. Enhanced antitumor efficacy of telomerase-selective oncolytic adenoviral agent OBP-401 with docetaxel: preclinical evaluation of chemovirotherapy. *Int J Cancer* 2006;119:432–40.
 15. Riley T, Sontag E, Chen P, Levine A. Transcriptional control of human p53-regulated genes. *Nat Rev Mol Cell Biol* 2008;9:402–12.
 16. Lefebvre JL. Current clinical outcomes demand new treatment options for SCCHN. *Ann Oncol* 2005;16 Suppl 6:vi7–12.
 17. Endo Y, Sakai R, Ouchi M, et al. Virus-mediated oncolysis induces danger signal and stimulates cytotoxic T-lymphocyte activity via proteasome activator upregulation. *Oncogene* 2008;27:2375–81.
 18. Ito H, Aoki H, Kühnel F, et al. Autophagic cell death of malignant glioma cells induced by a conditionally replicating adenovirus. *J Natl Cancer Inst* 2006;98:625–36.
 19. Sarker D, Workman P. Pharmacodynamic biomarkers for molecular cancer therapeutics. *Adv Cancer Res* 2007;96:213–68.
 20. Fidler IJ. Rationale and methods for the use of nude mice to study the biology and therapy of human cancer metastasis. *Cancer Metastasis Rev* 1986;5:29–49.
 21. Fidler IJ, Naito S, Pathak S. Orthotopic implantation is essential for the selection, growth and metastasis of human renal cell cancer in nude mice. *Cancer Metastasis Rev* 1990;9:149–65.
 22. Killian JJ, Radinsky R, Fidler IJ. Orthotopic models are necessary to predict therapy of transplantable tumors in mice. *Cancer Metastasis Rev* 1998;17:279–84.
 23. Langer C.J. Targeted therapy in head and neck cancer: state of the art 2007 and review of clinical applications. *Cancer* 2008;112:2635–45.
 24. Widakowich C, de Castro G, Jr., de Azambuja E, Dinh P, Awada A. Review: side effects of approved molecular targeted therapies in solid cancers. *Oncologist* 2007;12:1443–55.
 25. Fujiwara T, Tanaka N, Nemunaitis J, et al. Phase I trial of intratumoral administration of OBP-301, a novel telomerase-specific oncolytic virus, in patients with advanced solid cancer: Evaluation of biodistribution and immune response. 2008 ASCO Annual Meeting Proceedings. *J Clin Oncol* 2008;26:3572.
 26. Del Vecchio S, Zannetti A, Fonti R, Pace L, Salvatore M. Nuclear imaging in cancer theranostics. *Q J Nucl Med Mol Imaging* 2007;51:152–63.

A Novel Antiangiogenic Effect for Telomerase-Specific Virotherapy through Host Immune System¹

Yoshihiro Ikeda,* Toru Kojima,* Shinji Kuroda,* Yoshikatsu Endo,* Ryo Sakai,* Masayoshi Hioki,* Hiroyuki Kishimoto,* Futoshi Uno,* Shunsuke Kagawa,*[†] Yuichi Watanabe,[‡] Yuuri Hashimoto,[‡] Yasuo Urata,[‡] Noriaki Tanaka,* and Toshiyoshi Fujiwara^{2*†}

Soluble factors in the tumor microenvironment may influence the process of angiogenesis; a process essential for the growth and progression of malignant tumors. In this study, we describe a novel antiangiogenic effect of conditional replication-selective adenovirus through the stimulation of host immune reaction. An attenuated adenovirus (OBP-301, Telomelysin), in which the human telomerase reverse transcriptase promoter element drives expression of E1 genes, could replicate in and cause selective lysis of cancer cells. Mixed lymphocyte-tumor cell culture demonstrated that OBP-301-infected cancer cells stimulated PBMC to produce IFN- γ into the supernatants. When the supernatants were subjected to the assay of in vitro angiogenesis, the tube formation of HUVECs was inhibited more efficiently than recombinant IFN- γ . Moreover, in vivo angiogenic assay using a membrane-diffusion chamber system s.c. transplanted in *nu/nu* mice showed that tumor cell-induced neovascularization was markedly reduced when the chambers contained the mixed lymphocyte-tumor cell culture supernatants. The growth of s.c. murine colon tumors in syngenic mice was significantly inhibited due to the reduced vascularity by intratumoral injection of OBP-301. The antitumor as well as antiangiogenic effects, however, were less apparent in SCID mice due to the lack of host immune responses. Our data suggest that OBP-301 seems to have antiangiogenic properties through the stimulation of host immune cells to produce endogenous antiangiogenic factors such as IFN- γ . *The Journal of Immunology*, 2009, 182: 1763–1769.

Angiogenesis is the development of new capillaries from preexisting capillary blood vessels and is necessary for the growth of solid tumors beyond 1–2 mm in diameter (1). Targeting the angiogenic process is therefore regarded as a promising strategy in cancer therapy. Angiogenesis consists of dissolution of the basement membrane, migration and proliferation of endothelial cells, canalization, branching and formation of vascular loops, and formation of a basement membrane (2). These steps might be regulated by the local balance between the amount of angiogenic stimulators and inhibitors (3–5). As cells undergo malignant transformation, angiogenic mitogens such as vascular endothelial growth factor (VEGF),³ basic fibroblast growth factor, platelet-derived epithelial cell growth factor, and TGF become dominant, causing the aberrant angiogenesis. In contrast, many endogenous angio-

genic inhibitors such as platelet factor 4, thrombospondin 1, angiostatin, endostatin, various antiangiogenic peptides, hormone metabolites, and cytokines constitutively suppress angiogenesis in normal tissues (6). These scenarios suggest the possibility that endogenous angiogenic inhibitors that outweigh the stimulators could turn off the angiogenic switch.

Recent studies have demonstrated that the tumor microenvironment, which orchestrates with the host immune system, is a critical component of both tumor progression and tumor suppression (7). Indeed, the production of cytokines at tumor sites can either stimulate or inhibit tumor growth and progression (8). These findings provide a unique therapeutic opportunity based on selective and locoregional production of endogenous antitumor mediators such as angiogenic inhibitors. We reported previously that telomerase-specific replication-competent adenovirus (Telomelysin, OBP-301), in which the human telomerase reverse transcriptase promoter element drives the expression of *E1A* and *E1B* genes linked with an internal ribosomal entry sequence, induced selective E1 expression and efficiently killed human cancer cells, but not normal human fibroblasts (9–12). Although the precise molecular mechanism of OBP-301-induced cell death is still unclear, the process of oncolysis is morphologically distinct from apoptosis and necrosis. We found that tumor cells killed by OBP-301 infection could stimulate host immune cells more efficiently compared with chemotherapeutic drug-induced apoptotic cells and necrotic cells by freeze/thaw, thus enhancing the antitumor immune response (13). These results suggest that oncolytic virus is effective not only as a direct cytotoxic drug but also as an immunostimulatory agent that could modify the tumor microenvironment.

In the present article, we explored whether OBP-301-infected oncolytic cells can activate host immune cells and influence tumor

*Division of Surgical Oncology, Department of Surgery, Okayama University Graduate School of Medicine, Dentistry and Pharmaceutical Sciences, Okayama, [†]Center for Gene and Cell Therapy, Okayama University Hospital, Okayama, and [‡]Oncology BioPharma, Tokyo, Japan

Received for publication July 22, 2008. Accepted for publication November 26, 2008.

The costs of publication of this article were defrayed in part by the payment of page charges. This article must therefore be hereby marked *advertisement* in accordance with 18 U.S.C. Section 1734 solely to indicate this fact.

¹ This work was supported by Grants-in-Aid from the Ministry of Education, Science, and Culture, Japan (to T.F.) and grants from the Ministry of Health and Welfare, Japan (to T.F.).

² Address correspondence and reprint requests to Dr. Toshiyoshi Fujiwara, Center for Gene and Cell Therapy, Okayama University Hospital, 2-5-1 Shikata-cho, Okayama 700-8558, Japan. E-mail address: toshi_f@md.okayama-u.ac.jp

³ Abbreviations used in this paper: VEGF, vascular endothelial growth factor; MLTC, mixed lymphocyte-tumor cell culture; MOI, multiplicity of infection.

Copyright © 2009 by The American Association of Immunologists, Inc. 0022-1767/09/\$2.00

cell-mediated angiogenesis *in vitro* and *in vivo*. Antineoplastic effect of intratumoral administration of OBP-301 on s.c. murine colon tumors transplanted was compared in syngenic immunocompetent mice and SCID mice. Finally, we examined the effect of neutralizing anti-IFN- γ Ab on OBP-301-mediated antiangiogenic potential *in vivo*.

Materials and Methods

Cell lines and reagents

The human colorectal carcinoma cell lines SW620 (HLA-A02/A24) and the murine colon adenocarcinoma cell line Colon-26 were maintained *in vitro* in RPMI 1640 supplemented with 10% FCS, 100 U/ml penicillin, and 100 mg/ml streptomycin. Recombinant human IFN- γ was purchased from Peprotech.

Mice

Female BALB/c (BALB/cAnNCrCrIj), BALB/c *nu/nu* (CAnN.Cg-Foxn1⁰/CrIj), and SCID (CB17/1cr-Prkdc^{scid}/CrIj) mice, 5–6 wk of age, were purchased from Charles River Japan Breeding Laboratories. Animals were housed under specific pathogen-free conditions in accordance with the guidelines of the Institutional Animal Care and Use Committee.

Adenovirus

The recombinant replication-selective, tumor-specific adenovirus vector OBP-301 (Telomelysin), in which the human telomerase reverse transcriptase promoter element drives the expression of *E1A* and *E1B* genes linked with an internal ribosomal entry sequence, was constructed and previously characterized (9–12). The virus was purified by CsCl₂ step gradient ultracentrifugation followed by CsCl₂ linear gradient ultracentrifugation.

Cell viability assay

XTT assay was performed to measure cell viability. Briefly, cells were plated on 96-well plates at 5×10^3 per well 24 h before treatment and then infected with OBP-301. Cell viability was determined at the times indicated by using a Cell Proliferation kit II (Roche Molecular Biochemicals) according to the protocol provided by the manufacturer.

Mixed lymphocyte-tumor cell culture (MLTC) and cytokine production assay

For MLTC, SW620 tumor cells were infected with OBP-301 at a multiplicity of infection (MOI) of 10, washed three times in PBS 72 h after infection, and then cocultured with PBMC at a ratio of 1:40. The supernatant was collected at the indicated times and stored at -80°C until assay. The concentration of IFN- γ was measured with ELISA kits (BioSource International).

In vitro angiogenesis assay

In vitro angiogenesis was assessed based on the formation of capillary-like structures by HUVECs cocultured with human diploid fibroblasts according to the instructions provided with the angiogenesis kit (Kurabo). In brief, the HUVECs were incubated in a medium containing the diluted supernatants of MLTC or recombinant IFN- γ in the presence or absence of VEGF (10 ng/ml). The medium was replaced at days 4, 7, and 9. At day 11, the HUVECs were fixed and stained by using an anti-human CD31 Ab (Kurabo) according to the instructions provided. The formation of the capillary network was observed with a microscope at a magnification of $\times 40$.

In vivo assay for tumor angiogenesis

In vivo angiogenesis was determined using the dorsal air-sac method (14). Briefly, 2×10^6 SW620 cells were suspended in PBS containing the diluted supernatants of MLTC or control medium, and placed into round-shaped chambers that consisted of a ring covered with cellulose ester filters (pore size, 0.45 μm ; Millipore) on both sides. These chambers were implanted into a dorsal air sac produced in female BALB/c *nu/nu* mice by the injection of 10 ml of air. Five mice in each group were sacrificed on day 5, and the formation of a dense capillary network in s.c. regions was examined under a dissecting microscope. The neovascularization was assessed semiquantitatively by counting the number of cork screw vessels. For each slide, a total of three fields at a magnification of $\times 4$ were selected at random, and the scores were averaged.

In vivo tumor growth and determination of microvessels

Female BALB/c and SCID mice were s.c. implanted with 2×10^6 Colon-26 cells. When tumors grew to ~ 5 –6 mm in diameter, the mice were randomly assigned into three groups and a 100 μl of solution containing 1×10^8 PFU of dl312 or OBP-301, or PBS was injected into the tumor on days 1, 3, and 5. Tumors were measured for perpendicular diameters every 3 or 4 days, and tumor volume (in cubic millimeters) was calculated using the following formula: $a \times b^2 \times 0.5$, where a is the longest diameter, b is the shortest diameter, and 0.5 is a constant to calculate the volume of an ellipsoid. For histological analysis, 2 wk after treatment, the tumors were harvested, embedded in Tissue Tek (Sakura), cut into 5 μm -thick sections, and assessed by a standard H&E and immunohistochemical staining using a rat anti-mouse mAb against CD31 (BD Pharmingen). The experimental protocol was approved by the Ethics Review Committee for Animal Experimentation of Okayama University Graduate School of Medicine, Dentistry, and Pharmaceutical Sciences.

In vivo inhibition of IFN- γ with neutralizing Abs

For neutralizing IFN- γ , mice were i.p. administered 200 μg of rat anti-mouse IFN- γ mAb (XMG1.2; BD Pharmingen) 1 day before the first injection of OBP-301 and on days 1 and 3 after the first injection. Control mice received i.p. administration of isotype-matched rat IgG1 (BD Pharmingen).

Statistical analysis

Determination of significant differences among groups was assessed by calculating the value of Student's *t* test using the original data analysis. Statistical significance was defined at $p < 0.01$.

Results

Effect of OBP-301-infected human colorectal cancer cells on PBMC *in vitro*

First, we examined whether OBP-301 infection affects the viability of human colorectal cancer cells using the XTT assay. SW620 cells were either mock-infected with culture medium or infected with OBP-301 at an MOI of 1 or 10. As shown in Fig. 1A, OBP-301 infection induced death of SW620 cells in a dose-dependent manner. Next, we examined the ability of OBP-301-infected oncolytic cells to stimulate PBMC in MLTC. For this purpose, SW620 cells (HLA-A02/A24) treated with 10 MOI of OBP-301 for 72 h were cocultured with HLA-matched PBMC obtained from HLA-A24⁺ healthy volunteers at a ratio of 1:40. The production of IFN- γ in the supernatants was then explored by ELISA analysis at the indicated time points. PBMC incubated with OBP-301-infected oncolytic SW620 cells secreted large amounts of IFN- γ as early as 24 h after MLTC, whereas PBMC alone induced little IFN- γ secretion (Fig. 1B). The maximum level of IFN- γ was ~ 250 pg/ml. We previously confirmed that addition of OBP-301 alone without target tumor cells did not affect the cytokine secretion from PBMC into the supernatant, indicating that infection of OBP-301 itself had no apparent effect on PBMC (13). These results suggest that PBMC stimulated with oncolytic tumor cells preferentially secrete high-level IFN- γ .

Inhibition of *in vitro* and *in vivo* angiogenesis by MLTC supernatants with OBP-301-infected human tumor cells

In the next step, we investigated the effects of MLTC supernatants with oncolytic SW620 tumor cells and HLA-matched PBMC on VEGF-induced angiogenesis *in vitro*. The addition of VEGF enhanced the formation of vascular-like structures of HUVECs, although tubule formation was almost absent without VEGF. This VEGF-induced angiogenesis was completely impaired by the addition of MLTC supernatants even at 1/4 dilution (Fig. 2). In contrast, although MLTC supernatants were confirmed to contain ~ 250 pg/ml IFN- γ , 10-fold more concentration of recombinant IFN- γ was needed to attenuate the tubule formation close to basal levels. The supernatants of PBMC

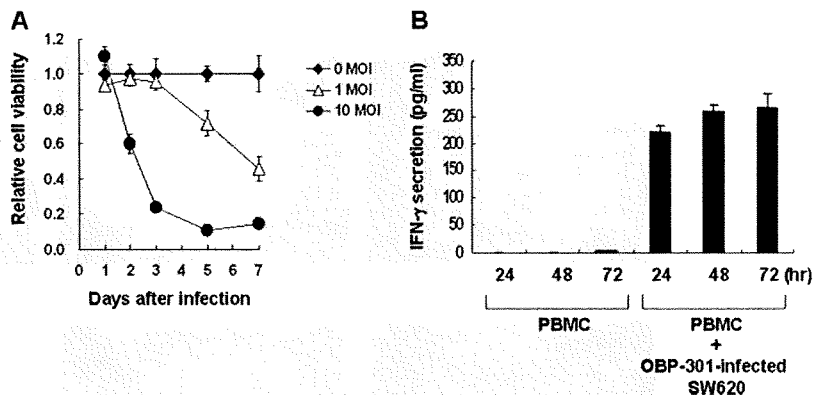


FIGURE 1. In vitro cytopathic effects of OBP-301 and IFN- γ secretion by oncolytic cell-stimulated PBMC. *A*, SW620 human colorectal cancer cells were infected with OBP-301 at indicated MOI values, and surviving cells were quantitated over 7 days by XTT assay. The cell viability of mock-treated cells on day 1 was considered 1.0, and the relative cell viability was calculated. Data are mean \pm SD of triplicate experiments. *B*, IFN- γ concentrations in the supernatants of MLTC analyzed by ELISA. SW620 cells were treated with 10 MOI of OBP-301 for 72 h, and then cocultured with PBMCs obtained from HLA-A24⁺ healthy volunteers for the indicated time periods in MLTC. The culture supernatants were harvested and tested by ELISA for IFN- γ concentrations. As a control, the supernatants of PBMC alone were also examined. Data are mean \pm SD of triplicate experiments.

alone had no effect on in vitro angiogenesis. These results suggest that MLTC supernatants may contain more antiangiogenic factors in addition to IFN- γ .

We also assessed whether MLTC supernatants inhibited in vivo angiogenesis induced by human cancer cells. SW620 cells in PBS containing supernatants of OBP-301-infected SW620 cells, PBMC, or both, which were packed into membrane chambers, were implanted into a dorsal air sac produced in *nu/nu* mice. The chambers consisted of membranes that allowed the passage of macromolecules such as IFN- γ , but not cells. Five days after implantation, neovascularization, as demonstrated by the development of capillary networks and curled microvessels in addition to the preexisting vessels, occurred in the dorsal subcutis touched by the chamber, which contained SW620 cells alone. The addition of MLTC supernatants, however, reduced the size and tortuosity of the preexisting vessels, and significantly reduced the development of curled microvessels (Fig. 3). Although the preexisting vessels became thinner by supernatants of OBP-301-infected SW620 cells or PBMC, the number of curled microvessels, which is characteristic of tumor neovasculature, was consistent in these two groups with that in the group compared with SW620 cells alone. Thus, MLTC supernatants exhibited a profound antiangiogenic activity in vivo.

Involvement of host immune activity on antiangiogenic effect of OBP-301

The finding that OBP-301-infected tumor cells stimulated PBMC to produce antiangiogenic factors prompted us to study whether immunodeficiency of host animals could affect the antitumor effect of OBP-301 in vivo. When 2×10^6 Colon-26 murine colon adenocarcinoma cells were inoculated s.c. into BALB/c and SCID mice, palpable tumors appeared in 100% of the mice within 2 wk after tumor injection. Fourteen days after tumor inoculation, animals bearing Colon-26 tumors with a diameter of 5–6 mm were treated with the direct intratumoral injection of 10^8 PFU OBP-301 every 2 days for three cycles. As shown in Fig. 4, treatment with OBP-301 resulted in a significant growth suppression compared with tumors injected with PBS at least for 12 days starting on day 4 after last virus injection ($p < 0.01$) in BALB/c mice; however, OBP-301-mediated antitumor effect was partially impaired in SCID mice, as significant inhibition was observed only for 6 days starting on day 10. Intratumoral injection of replication-deficient dl312 adenovirus had no effect on the tumor growth in BALB/c or SCID mice (data not shown). These results indicate the partial involvement of the host immune system in the OBP-301-mediated antitumor effect.

FIGURE 2. Inhibition of in vitro angiogenesis by the supernatants of OBP-301-infected oncolytic cells and PBMC. HUVECs were incubated in a medium containing the supernatants of MLTC obtained 72 h after coculture with OBP-301-infected oncolytic cells and PBMC or recombinant IFN- γ in the presence or absence of VEGF (10 ng/ml). The formation of the capillary network was confirmed by staining with anti-human CD31 Ab on day 11. Representative images depicting formation of capillary-like tube structures by HUVECs are shown. Original magnification is at $\times 40$.

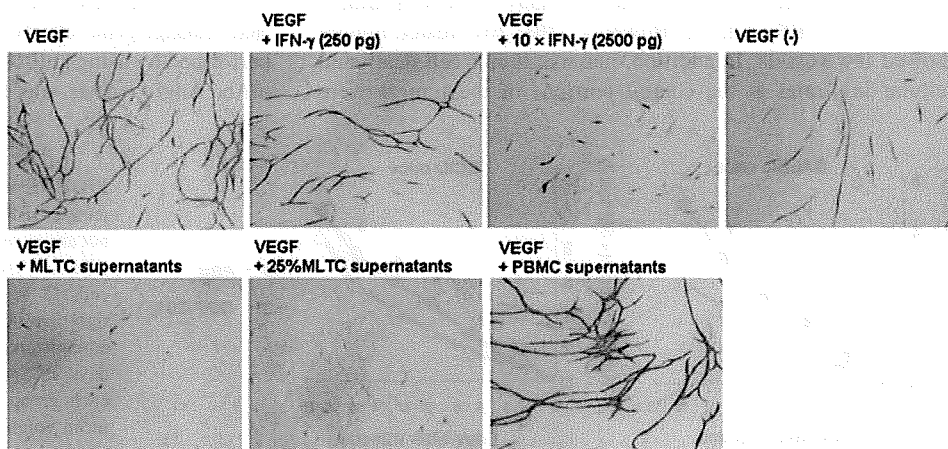
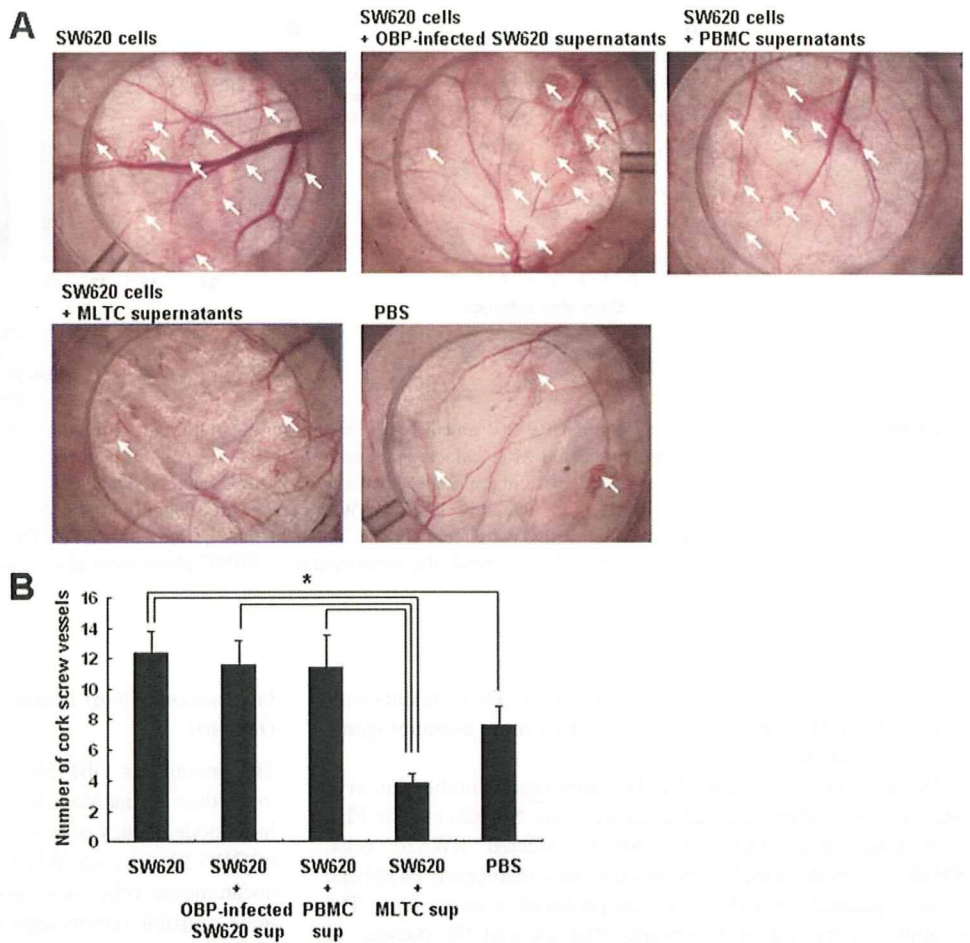


FIGURE 3. Inhibition of tumor cell-mediated in vivo angiogenesis by the supernatants of OBP-301-infected oncolytic cells and PBMC. *A*, SW620 human colorectal tumor cells at a density of 2×10^6 were placed in a diffusion chamber in PBS containing the diluted supernatants of MLTC obtained 72 h after coculture with OBP-301-infected oncolytic cells and PBMC or control mediums, and it was implanted into a dorsal air space produced in BALB/c *nu/nu* mice on day 0. Mice were sacrificed on day 5, and the chamber was removed from the s.c. tissue. A new ring without filters was placed on the same site to mark the position of the chamber. The capillary networks developed inside the rings were photographed to determine the effect of treatments. Representative images of treatment groups are shown. Curled microvessels are shown (arrow). *B*, The number of cork screw vessels was semiquantitatively counted to assess the neovascularization. Data are mean \pm SD. *, $p < 0.01$. Similar results were observed in two independent experiments conducted in triplicate.



Antiangiogenic effect of OBP-301 on syngenic and immunodeficient murine tumor models

When Colon-26 s.c. tumors implanted in BALB/c mice were injected with PBS, replication-deficient dl312 adenovirus, or OBP-301. Macroscopically, tumors treated with OBP-301 were consistently smaller than those of the other two cohorts of mice 14 days after last virus injection (Fig. 5A). Furthermore, a reddish area was noted on the tumor surface on two of six mice treated with OBP-301, indicating virus-induced intratumoral necrosis of tumor cells in vivo.

To better understand the mechanisms underlying the induction of necrosis following OBP-301 treatment, histologic and immunohistochemical analyses were performed on Colon-26 tumors harvested 14 days after last injection. A standard H&E staining demonstrated the presence of many vessels in tumors injected with PBS or dl312. However, OBP-301-treated tumors showed few vessels. In addition, massive tumor cell death and cellular infiltrates at the central portions of the tumors were

observed where OBP-301 was injected (Fig. 5B). Immunohistochemical staining of tumor sections with the Ab for CD31 Ag, an endothelial cell marker, also revealed that Colon-26 tumors injected with OBP-301 displayed very few and extremely small blood vessels (Fig. 5C). In contrast, OBP-301 injection could not apparently reduce the vessel numbers on Colon-26 tumors implanted in SCID mice (Fig. 5D). These in vivo studies demonstrated that inhibition of angiogenesis due to the stimulation of host immune system might be an important mechanism of OBP-301-mediated in vivo antitumor effect.

Contribution of in vivo IFN- γ production to the OBP-301-mediated antiangiogenic effects

Finally, to determine whether IFN- γ is involved in OBP-301-mediated antiangiogenic effects, in vivo neutralizing experiments were performed by using anti-IFN- γ mAb or isotype-matched control mAb. Angiogenesis was reduced by intratumoral injection of

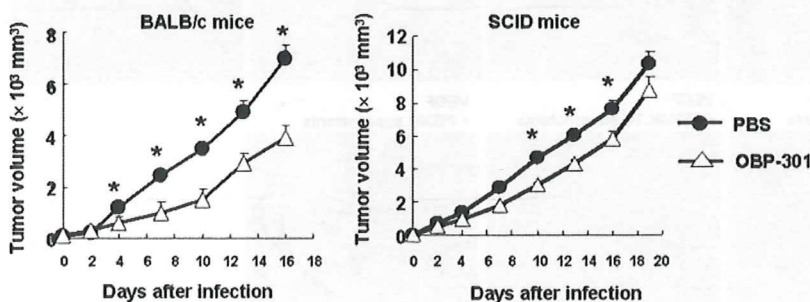


FIGURE 4. Antitumor effects of intratumorally injected OBP-301 against Colon-26 murine colon adenocarcinoma tumors in syngenic immunocompetent BALB/c and immunodeficient SCID mice. Colon-26 cells (2×10^6 cells/each) were injected s.c. into the right flank of mice. OBP-301 (1×10^8 PFU/body) was administered intratumorally for three cycles every 2 days. PBS was used as a control. Six mice were used in each group. Tumor growth was expressed by tumor mean volume \pm SD. *, $p < 0.01$.

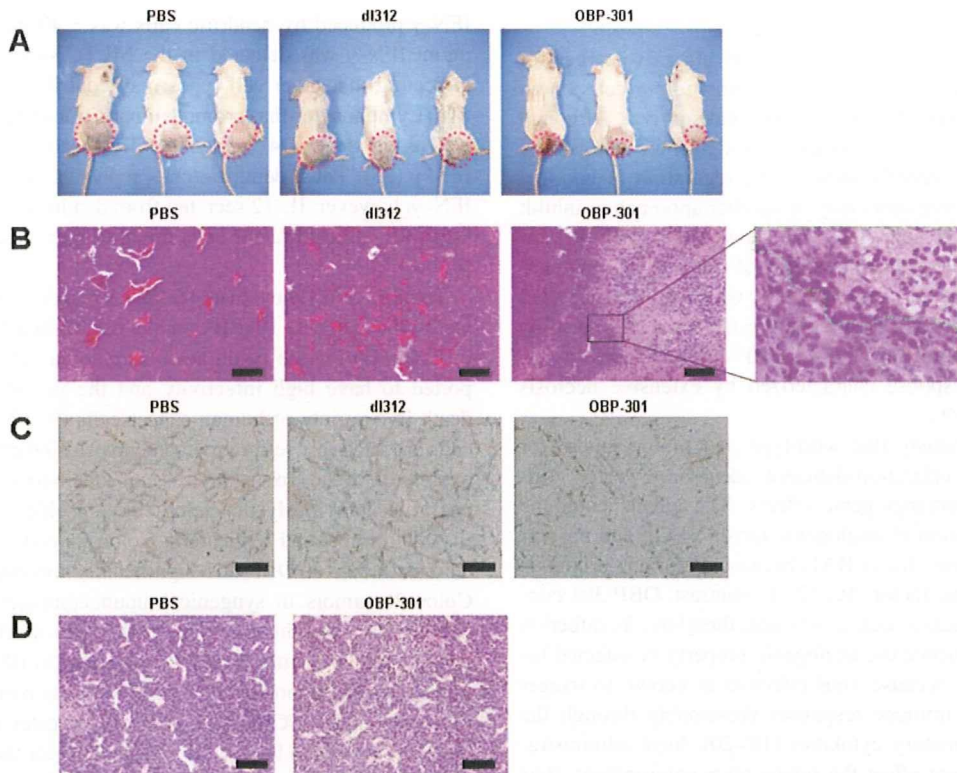


FIGURE 5. Macroscopic and histopathological analysis of Colon-26 tumors treated intratumorally with OBP-301. Colon-26 cells (2×10^6 cells/each) were injected s.c. into the right flank of syngenic BALB/c mice and SCID mice and OBP-301 (1×10^8 PFU/body) was administered intratumorally for three cycles every 2 days as described in Fig. 4. *A*, Macroscopic appearance of Colon-26 tumors on BALB/c mice 14 days after treatment. Note the reddish area on the tumor surface in two mice treated with OBP-301. *B*, Tumor sections were obtained from BALB/c mice 14 days after final administration of OBP-301. Frozen sections of tumors were stained with H&E. Scale bar represents $100 \mu\text{m}$, and magnification is $\times 100$. Magnified view of the boxed region in *B* is shown. The area with cellular infiltrates is indicated with the green dotted line. *C*, Blood vessel formation in Colon-26 tumors injected with OBP-301. Frozen sections of the tumors were also probed with an Ab against CD31. Scale bar represents $50 \mu\text{m}$, and magnification is $\times 200$. *D*, Tumor sections were obtained from SCID mice 14 days after final administration of OBP-301. Frozen sections of tumors were stained with H&E. Scale bar represents $100 \mu\text{m}$, and magnification is at $\times 100$ magnification.

OBP-301 on Colon-26 tumors; this antiangiogenic effect, however, could be partially inhibited in the presence of anti-IFN- γ mAb (Fig. 6). Treatment with control IgG1 had no effect on the

antiangiogenic effects of OBP-301. These results suggest that IFN- γ may be one of the important factors for OBP-301 to inhibit angiogenesis in vivo.

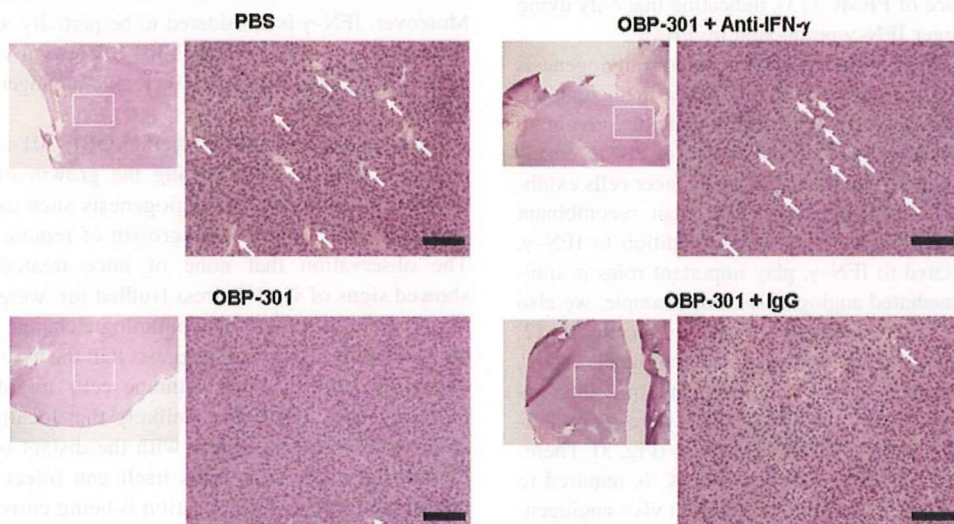


FIGURE 6. Effects of anti-IFN- γ Abs on angiogenesis in Colon-26 tumors. Colon-26 cells (2×10^6 cells/each) were injected s.c. into the right flank of syngenic BALB/c mice and OBP-301 (1×10^8 PFU/body) was administered intratumorally for three cycles every 2 days as described in Fig. 4. Mice were administered $200 \mu\text{g}$ of anti-IFN- γ mAb (XMG1.2) i.p. to neutralize IFN- γ 1 day before the first injection of OBP-301 and on days 1 and 3 after the first injection. Control mice received i.p. administration of isotype-matched rat IgG1 or PBS. Frozen sections of tumors obtained 14 days after final administration of OBP-301 were stained with H&E. Magnified view (*right*) of the boxed region (*left*). Microvessels are shown (arrow). Scale bar represents $50 \mu\text{m}$, and magnification is at $\times 200$.

Discussion

The tumor vasculature provides a new and attractive target for cancer therapy because of the reliance of most tumor cells on an adequate vascular supply for their growth and survival. Although the beneficial effects of novel antiangiogenic agents such as bevacizumab have been recently shown (15), regulation of endogenous antiangiogenic mediators may be another approach to inhibit angiogenesis. In the present study, we showed that OBP-301 infection and replication induced cytolysis of tumor cells with subsequent stimulation of host immune cells, which in turn inhibited tumor angiogenesis *in vivo*. Treatment of established murine colon tumors with intratumoral injection of OBP-301 resulted in a significant antitumor response characterized by extensive necrosis and reduced vascularity.

We reported previously that wild-type *p53* tumor suppressor gene transfer by a replication-deficient adenovirus vector (Ad-vexin) could have antiangiogenic effects. The effects could be through down-regulation of angiogenic factor VEGF and up-regulation of antiangiogenic factor BAI1 because tumor *p53* protein is a potent transcriptional factor (16, 17). In contrast, OBP-301 contains no therapeutic genes such as *p53* and, therefore, its infection may not directly influence the angiogenic property of infected tumor cells. However, because viral infection is known to trigger innate and adaptive immune responses presumably through the release of proinflammatory cytokines (18–20), local administration of OBP-301 might affect the tumor microenvironment, thus explaining the potential therapeutic benefit on tumor angiogenesis. In fact, dying tumor cells infected with OBP-301 promoted the production of Th1 cytokines by PBMC such as IFN- γ , which is one of the most potent antiangiogenic factors (21, 22) (Fig. 1). Viral infection itself has been reported to activate dendritic cells to secrete pro- or anti-inflammatory cytokines (23); our preliminary experiments, however, demonstrated that OBP-301 alone had no effect on cytokine production by PBMC (13), indicating that OBP-301 itself may be less infective or stimulatory to PBMC. The result is consistent with our previous finding that OBP-301 attenuated replication as well as cytotoxicity of human normal cells (9, 10). Moreover, OBP-301-infected tumor cells, but not untreated tumor cells, enhanced IFN- γ -inducible proteasome activator PA28 expression in the presence of PBMC (13), indicating that only dying tumor cells could trigger IFN- γ production by PBMC.

IFN- γ has been also known to inhibit tumor angiogenesis through the subsequent stimulation of secondary mediators, including monokine induced by IFN- γ and IFN-inducible protein 10 (24). Indeed, the observation that the supernatants of PBMC cocultured with OBP-301-infected human colorectal cancer cells exhibited a more profound antiangiogenic effect than recombinant IFN- γ (Fig. 2) suggests that other factors in addition to IFN- γ , which may not be related to IFN- γ , play important roles in inhibition of tumor cell-mediated angiogenesis. For example, we also found that oncolytic cells stimulated PBMC to secrete IL-12, which is an inducer of IFN- γ as well as an antiangiogenic factor, into the culture supernatants (13). The supernatants of neither virus-infected tumor cells alone nor PBMC alone were more antiangiogenic compared with those of MLTC *in vivo* (Fig. 3). Therefore, the interaction of oncolytic cells and PBMC is required to produce antiangiogenic mediators and to inhibit *in vivo* angiogenesis following OBP-301 treatment. The question what kind of cells produce mediators for antiangiogenic effects is of interest. We reported previously that OBP-301 replication produced the endogenous danger signaling molecule, uric acid, in infected human tumor cells, which in turn stimulated dendritic cells to produce IFN- γ as well as IL-12 into the supernatants (13). The amount of

IFN- γ produced by dendritic cells was ~ 40 pg/ml, although 250 pg/ml IFN- γ was detected in the MLTC supernatants (Fig. 1B), indicating that other cell types may contribute to IFN- γ production. Lymphocytes that promote innate immunity (i.e., NK cells) as well as classical CD4⁺ and CD8⁺ T cells are also known to produce IFN- γ (25). Thus, dendritic cells represent one of the sources of IFN- γ ; however, IL-12 secreted from dendritic cells activated with OBP-301-infected tumor cells might trigger these cells to produce IFN- γ .

To more directly evaluate the antiangiogenic effect of OBP-301, we used a syngenic BALB/c model established by s.c. inoculation of Colon-26 murine colon adenocarcinoma cells. OBP-301 is reported to have high infectivity and the potential to induce cell death in a variety of human cancer cells (9–12), whereas murine cells are relatively refractory to adenovirus infection due to the low expression of the coxsackievirus and adenovirus receptor. We have confirmed previously that telomerase-specific oncolytic adenovirus could infect and replicate in Colon-26 cells (12). Intratumoral administration of OBP-301 significantly inhibited the growth of Colon-26 tumors in syngenic immunocompetent BALB/c mice, although the magnitude of suppression was much less when compared with that in human tumor xenografts (9, 10). The finding that tumor growth suppression by OBP-301 was partially inhibited in immunodeficient SCID mice (Fig. 4) indicates that the host immune system could be partially responsible for the antitumor effect of OBP-301. Histopathologic analysis revealed that the presence of the immune cell infiltrates and the massive necrosis in Colon-26 tumors are exclusively due to the tumor-specific viral replication because dl312-injected tumors showed neither cellular infiltrates nor tissue damages (Fig. 5B). In view of the fact that a cellular infiltration could be still observed as late as 14 days after the last OBP-301 injection, immune responses are likely to be induced by oncolytic tumor cells. Furthermore, as expected, tumors injected with OBP-301 formed less blood vessels than mock- or dl312-treated tumors (Fig. 5, B and C), suggesting that inhibition of angiogenesis by infiltrating cell-secreted mediators partially elicits the antitumor activity of OBP-301. In contrast, antiangiogenic effect of OBP-301 was impaired in SCID mice (Fig. 5D), indicating that host immune cells are necessary for this function of OBP-301. Moreover, IFN- γ is considered to be partially responsible for the antiangiogenic effects of OBP-301 because *in vivo* neutralization of IFN- γ by anti-IFN- γ mAb increased angiogenesis on Colon-26 tumors (Fig. 6).

It remains to be studied whether OBP-301-infected oncolytic cells are capable of inhibiting the growth of distant tumors. Circulating inhibitors of angiogenesis such as angiostatin and endostatin can suppress the growth of remote metastases (26). The observation that none of mice treated with OBP-301 showed signs of viral distress (ruffled fur, weight loss, lethargy, or agitation) as well as histopathologic changes in any organs at autopsy (data not shown) suggests that the cytokine secretion by oncolytic cell-stimulated immune cells might be local rather than systemic. Thus, it is unlikely that locally produced antiangiogenic factors interfere with the distant tumor growth, although the circulating virus itself can infect and replicate in metastatic tumors. This question is being currently investigated in our laboratory.

In conclusion, we provide for the first time evidence that oncolytic virotherapy induces novel antiangiogenic effect by stimulating host immune cells to produce antiangiogenic mediators such as IFN- γ . Our data suggest that the antitumor effect of OBP-301 might be both direct and indirect.

Acknowledgments

We thank Hitoshi Kawamura and Daiju Ichimaru for helpful discussion. We also thank Yoshiko Shirakiya, Nobue Mukai, and Tomoko Sueishi for excellent technical assistance.

Disclosures

The authors have no financial conflict of interest.

References

- Folkman, J. 1985. Tumor angiogenesis. *Adv. Cancer Res.* 43: 175–203.
- Ausprunk, D. H., and J. Folkman. 1977. Migration and proliferation of endothelial cells in preformed and newly formed blood vessels during tumor angiogenesis. *Microvasc. Res.* 14: 53–65.
- Fidler, I. J., and L. M. Ellis. 1994. The implications of angiogenesis for the biology and therapy of cancer metastasis. *Cell* 79: 85–88.
- Folkman, J. 1995. Angiogenesis in cancer, vascular, rheumatoid and other disease. *Nat. Med.* 1: 27–31.
- Hanahan, D., and J. Folkman. 1996. Patterns and emerging mechanisms of the angiogenesis switch during tumorigenesis. *Cell* 86: 353–364.
- Nyberg, P., L. Xie, and R. Kalluri. 2005. Endogenous inhibitors of angiogenesis. *Cancer Res.* 65: 3967–3979.
- de Visser, K. E., A. Eichten, and L. M. Coussens. 2006. Paradoxical roles of the immune system during cancer development. *Nat. Rev. Cancer* 6: 24–37.
- Lin, W. W., and M. Karin. 2007. A cytokine-mediated link between innate immunity, inflammation, and cancer. *J. Clin. Invest.* 117: 1175–1183.
- Kawashima, T., S. Kagawa, N. Kobayashi, Y. Shirakiya, T. Umeoka, F. Teraishi, M. Taki, S. Kyo, N. Tanaka, and T. Fujiwara. 2004. Telomerase-specific replication-selective virotherapy for human cancer. *Clin. Cancer Res.* 10: 285–292.
- Taki, M., S. Kagawa, M. Nishizaki, H. Mizuguchi, T. Hayakawa, S. Kyo, K. Nagai, Y. Urata, N. Tanaka, and T. Fujiwara. 2005. Enhanced oncolysis by a tropism-modified telomerase-specific replication-selective adenoviral agent OBP-405 ('Telomelysin-RGD'). *Oncogene* 24: 3130–3140.
- Umeoka, T., T. Kawashima, S. Kagawa, F. Teraishi, M. Taki, M. Nishizaki, S. Kyo, K. Nagai, Y. Urata, N. Tanaka, and T. Fujiwara. 2004. Visualization of intrathoracically disseminated solid tumors in mice with optical imaging by telomerase-specific amplification of a transferred green fluorescent protein gene. *Cancer Res.* 64: 6259–6265.
- Kishimoto, H., T. Kojima, Y. Watanabe, S. Kagawa, T. Fujiwara, F. Uno, F. Teraishi, S. Kyo, H. Mizuguchi, Y. Urata, et al. 2006. In vivo imaging of lymph node metastasis with telomerase-specific replication-selective adenovirus. *Nat. Med.* 12: 1213–1219.
- Endo, Y., R. Sakai, M. Ouchi, H. Onimatsu, M. Hioki, S. Kagawa, F. Uno, Y. Watanabe, Y. Urata, N. Tanaka, and T. Fujiwara. 2008. Virus-mediated oncolysis induces danger signal and stimulates cytotoxic-T-lymphocyte activity via proteasome activator upregulation. *Oncogene* 27: 2375–2381.
- Tanaka, N. G., N. Sakamoto, K. Inoue, H. Korenaga, S. Kadoya, H. Ogawa, and Y. Osada. 1989. Antitumor effects of an antiangiogenic polysaccharide from an *Arthrobacter* species with or without a steroid. *Cancer Res.* 49: 6727–6730.
- Pfeiffer, P., C. Qvortrup, and J. G. Eriksen. 2007. Current role of antibody therapy in patients with metastatic colorectal cancer. *Oncogene* 26: 3661–3678.
- Bouvet, M., L. M. Ellis, M. Nishizaki, T. Fujiwara, W. Liu, C. D. Bucana, B. Fang, J. J. Lee, and J. A. Roth. 1998. Wild-type p53 gene transfer down-regulates vascular endothelial growth factor expression and inhibits angiogenesis in human colon cancer. *Cancer Res.* 58: 2288–2292.
- Nishizaki, M., T. Fujiwara, T. Tanida, A. Hizuta, H. Nishimori, T. Tokino, Y. Nakamura, M. Bouvet, J. A. Roth, and N. Tanaka. 1999. Recombinant adenovirus expressing wild-type p53 is antiangiogenic: a proposed mechanism for bystander effect. *Clin. Cancer Res.* 5: 1015–1023.
- Lindenmann, J., and P. A. Klein. 1967. Viral oncolysis: increased immunogenicity of host cell antigen associated with influenza virus. *J. Exp. Med.* 126: 93–108.
- Sinkovics, J. G. 1991. Viral oncolysates as human tumor vaccines. *Int. Rev. Immunol.* 7: 259–287.
- Li, H., A. Dutuor, X. Fu, and X. Zhang. 2007. Induction of strong antitumor immunity by an HSV-2-based oncolytic virus in a murine mammary tumor model. *J. Gene Med.* 9: 161–169.
- Fathallah-Shaykh, H. M., L. J. Zhao, A. I. Kafrouni, G. M. Smith, and J. Forman. 2000. Gene transfer of IFN- γ into established brain tumors represses growth by antiangiogenesis. *J. Immunol.* 164: 217–222.
- Qin, Z., J. Schwartzkopff, F. Pradera, T. Kammertoens, B. Seliger, H. Pircher, and T. Blankenstein. 2003. A critical requirement of interferon γ -mediated angiostasis for tumor rejection by CD8⁺ T cells. *Cancer Res.* 63: 4095–4100.
- Ho, L. J., J. J. Wang, M. F. Shiao, C. L. Kao, D. M. Chang, S. W. Han, and J. H. Lai. 2001. Infection of human dendritic cells by Dengue virus causes cell maturation and cytokine production. *J. Immunol.* 166: 1499–1506.
- Horton, M. R., C. M. McKee, C. Bao, F. Liao, J. M. Farber, J. Hodge-DuFour, E. Pure, B. L. Oliver, T. M. Wright, and P. W. Noble. 1998. Hyaluronan fragments synergize with interferon- γ to induce the C-X-C chemokines mig and interferon-inducible protein-10 in mouse macrophages. *J. Biol. Chem.* 273: 35088–35094.
- Ikeda, H., L. J. Old, and R. D. Schreiber. 2002. The roles of IFN γ in protection against tumor development and cancer immunoediting. *Cytokine Growth Factor Rev.* 13: 95–109.
- Folkman, J. 2002. Role of angiogenesis in tumor growth and metastasis. *Semin. Oncol.* 29: 15–18.

Antiviral activity of cidofovir against telomerase-specific replication-selective oncolytic adenovirus, OBP-301 (Telomelysin)

Masaaki Ouchi · Hitoshi Kawamura · Yasuo Urata · Toshiyoshi Fujiwara

Received: 15 June 2008 / Accepted: 30 July 2008 / Published online: 27 August 2008
© Springer Science + Business Media, LLC 2008

Summary We constructed a replication-competent oncolytic adenovirus, OBP-301 (Telomelysin), in which human telomerase reverse transcriptase (hTERT) promoter drives E1 genes. OBP-301 is currently being used in a phase-I clinical trial for various types of tumors. Under such conditions, anti-adenoviral agents should be available for safety use against OBP-301 since any adenoviral viremia could cause severe adverse effects. Cidofovir (CDV) is an acyclic nucleoside phosphonate that has a broad antiviral activity against DNA viruses. Here, we examined the antiviral effects of CDV against OBP-301. The *in vitro* cytopathic effects of OBP-301 were suppressed by CDV. Moreover, CDV decreased the adenoviral E1A gene copy number after OBP-301 infection. These results suggest that CDV is a potentially useful antiviral agent for OBP-301.

Keywords hTERT · Adenovirus · Cidofovir · Oncolytic virus · Clinical trial

Introduction

Oncolytic adenoviruses have been developed for treatment of human cancer. These viruses are designed to replicate and selectively kill cancer cells but to have minimum effect on normal cells [1]. Two major approaches to generate selective

replication of viruses within tumor cells have been used [2, 3]. One is to delete genes that are critical for replication of the virus in normal cells but are dispensable for cancer cells such as ONYX-015 or $\Delta 24$ [4]. The other approach is the replacement of the promoter region that initiates viral replication genes to the promoter region of the genes active in cancer cells [2, 3]. Various genetic or epigenetic targets limited to cancer cells have been investigated and used for constructing oncolytic adenoviruses.

Human telomerase reverse transcriptase (hTERT) is an enzymatic subunit of human telomerase [5]. Telomerase is expressed in almost all cancer cells but not in all normal cells [6]. Therefore, telomerase is an attractive target for treatment of cancer. We constructed previously the attenuated adenovirus, OBP-301 (Telomelysin), in which adenoviral E1A and E1B genes are linked with internal ribosomal entry site under the control of the hTERT promoter. We reported that OBP-301 induced selective expression of E1A and E1B genes in many cancer cell lines and selectively replicated and lysed cancer cells but not normal cells [7–9]. OBP-301 is currently being tested in a phase-I clinical trial that includes various types of solid tumors. Although patients receiving this type of therapy become positive for anti-adenoviral neutralizing antibodies, those treated with OBP-301 could develop adenoviral viremia with potentially severe adverse effects. Thus, there is a need for anti-adenoviral agents for treatment of potential viremia in clinical trials of OBP-301.

One of the antiviral compounds is phosphonyl acyclic nucleotides, (S)-9-(3-hydroxy-2-phosphonometoxy propyl) cytosine dehydrate, also known as HPMPC (cidofovir, or CDV). CDV was developed for the treatment of viral infections and has a broad antiviral activity against DNA viruses, such as cytomegalovirus and adenoviruses (AdV). CDV exhibits potent inhibitory effects against several

M. Ouchi · H. Kawamura · Y. Urata
Oncolys BioPharma, Inc.,
Tokyo 106-0032, Japan

T. Fujiwara (✉)
Center for Gene and Cell Therapy, Okayama University Hospital,
Okayama 700-8558, Japan
e-mail: toshi_f@md.okayama-u.ac.jp

adenoviral serotypes in cell culture models [10]. Furthermore, CDV has been used clinically for AdV infections after bone marrow transplantation in immunodeficient patients [11]. Thus, we presumed that CDV could be a useful antiviral drug against OBP-301. In the present study, we examined the *in vitro* inhibitory effects of CDV against OBP-301 in human lung cancer cell lines.

Materials and methods

Cell culture, viruses, and chemicals

The human non-small lung cancer cell H1299 and lung cancer cell line A549 were purchased from American Type Culture Collection (ATCC). H1299 was cultured in RPMI 1640 medium supplemented with 10% FCS. A549 was cultured in DMEM F12 medium supplemented with 10% fetal calf serum (FCS). OBP-301 was constructed and characterized as described previously [7–9]. The human wild-type adenovirus type 5 (wt-Ad) was also used. VISTIDE™ (CDV injection) was purchased from Gilead Sciences (Foster City, CA).

Cell viability assay

Cells were seeded in 96-well plate at 1×10^3 cells per well and incubated at 37°C. After incubation, cells were infected with OBP-301 at a MOI of 1 (in H1299) and 5 (in A549) for 2 hours. The medium was aspirated and replaced with fresh medium containing 2% FCS and serially diluted CDV. Cell viability was determined by XTT assay 7 days after infection using Cell Proliferation Kit II (Roche Molecular Biochemicals) according to the protocol recommended by the manufacturer. Protection was determined by the following formula: Protection (%) = $\frac{\text{OD (AdV(+):CDV(+))} - \text{OD (AdV(+):CDV(-))}}{\text{OD (AdV(-):CDV(+))} - \text{OD (AdV(+):CDV(-))}} \times 100$. CC₅₀ (50% cytotoxic concentration) was defined as CDV concentration that inhibited relative cell viability to 0.5 without OBP-301 infection. EC₅₀ (50% effective concentration) was defined as CDV concentration that archived 50% protection.

Quantitative real-time PCR analysis

Cells were seeded in six-well plate at 2×10^5 cells per well. After overnight incubation at 37°C, the medium was aspirated, and cells were infected with OBP-301 or wt-Ad at a MOI of 10 for 2 hours at 37°C with gentle shaking every 15 minutes. After incubation, the cells were washed with PBS and placed in a medium containing serially diluted CDV (100, 20, 4, 0.8, 0.16 and 0 μM). The cells were harvested 24 hours later with Trypsin/EDTA and total

DNA was extracted using QIAamp™ DNA Mini Kit (Qiagen, Hilden, Germany). Viral E1A copy number was measured using LightCycler instruments and LightCycler Faststart DNAMaster SYBR Green I (Roche, Mannheim, Germany). EC₅₀ (E1A) was defined as the CDV concentration that inhibits the E1A ratio (with CDV/no CDV) to 0.5. Primers for E1A gene were: forward: 5'- CCTGTGTCTA GAGAATGCAA -3', reverse: 5'- ACAGCTCAAGTC CAAAGGTT - 3'. PCR amplification began with a 600-s of denaturation step at 95°C and then 40 cycles of denaturation at 95°C for 10 s, annealing at 60°C for 15 s, and extension at 72°C for 8 s.

Statistical analysis

The Student's *t*-test was used to compare differences. Statistical significance was defined when *p* was <0.05.

Results

In vitro cytopathic effect of OBP-301 on lung cancer cell lines

We reported previously that OBP-301 exhibited oncolytic activity against many types of human cancer cells [7–9]. To confirm this, we tested its cytopathic effects in cancer cell line *in vitro*. Human lung cancer cell lines, A549 and H1299, were infected with OBP-301 at various MOIs and numbers of living cells were measured by XTT assay (Fig. 1). At 5 days after infection, the majority of H1299 cells were killed by OBP-301 at MOI of 1 and 10, and approximately 70% of A549 cells were killed by OBP-301 at MOI of 50. These results confirmed that OBP-301 induced cell death in A549 and H1299 cells.

Inhibitory effects of CDV on the cytopathic effect of OBP-301

Next, we tested whether the cytopathic effect by OBP-301 on these cancer cells could be inhibited by CDV treatment. A549 and H1299 cells were infected with OBP-301 then treated with CDV at various concentrations. Cell viability was also determined by XTT assay. In the presence of the drug and virus, relative cell viability significantly increased in the presence of CDV at > 30 μM in A549 cells and > 40 μM in H1299 cells (*p*<0.01) (Fig. 2). Furthermore, inhibition of cell growth of each cell line was observed in the presence of CDV at > 100 μM. The calculated EC₅₀ values of CDV were 20.4 μM for H1299 and 35.9 μM for A549 cells, while the calculated CC₅₀ values were 146.4 μM for H1299 cells and 106.9 μM for A549 cells. Similar results were obtained by using ONYX-015 (see

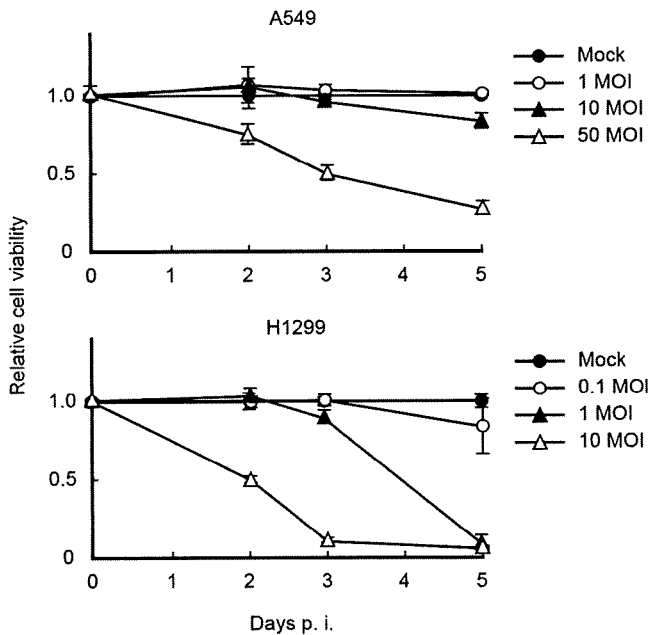


Fig. 1 Cytopathic effects of OBP-301 on H1299 and A549 lung cancer cell lines *in vitro*. Each cell was infected with OBP-301 at the indicated MOI and cell viability was evaluated by XTT assay (no virus=1.0). Data are mean±SD values

Introduction) and OBP-401, a modified OBP-301 that contains the GFP gene [12] (data not shown).

Inhibitory effects of CDV on viral replication of OBP-301

Finally, we examined whether CDV inhibits the replication of OBP-301 *in vitro*. We previously used two methods to

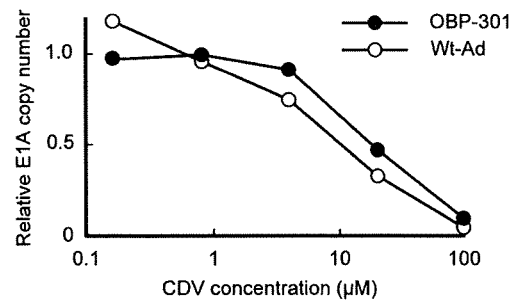


Fig. 3 Inhibition of OBP-301 replication in H1299 cells by CDV. Cells were infected with OBP-301 or wild-type AdV at MOI of 10, followed by the addition of CDV at the indicated concentrations. Cells were collected after 24 hours infection, total DNA was extracted, and viral E1A copy number was determined by quantitative real-time PCR analysis (with virus/no CDV=1.0)

quantify viral replication, biological plaque forming assay using 293 cells [7] and real-time PCR assay targeting adenoviral E1A sequence [8, 9], and found that both assays could detect viral replication similarly. H1299 cells were infected with OBP-301 or wt-Ad, followed by treatment with CDV. Wt-Ad was used for positive control in this assay since it had been reported that CDV had antiviral activity against wt-Ad. To measure the viral DNA, we quantified E1A copy number of cells infected with OBP-301 or wt-Ad by real-time PCR assay. CDV reduced the relative E1A copy number in both wt-Ad and OBP-301-infected cells and the effect was concentration-dependent, indicating that CDV inhibited viral replication of OBP-301 and wt-Ad in H1299 cells (Fig. 3). The calculated EC_{50} (E1A) value for OBP-301 was 19.55 μ M.

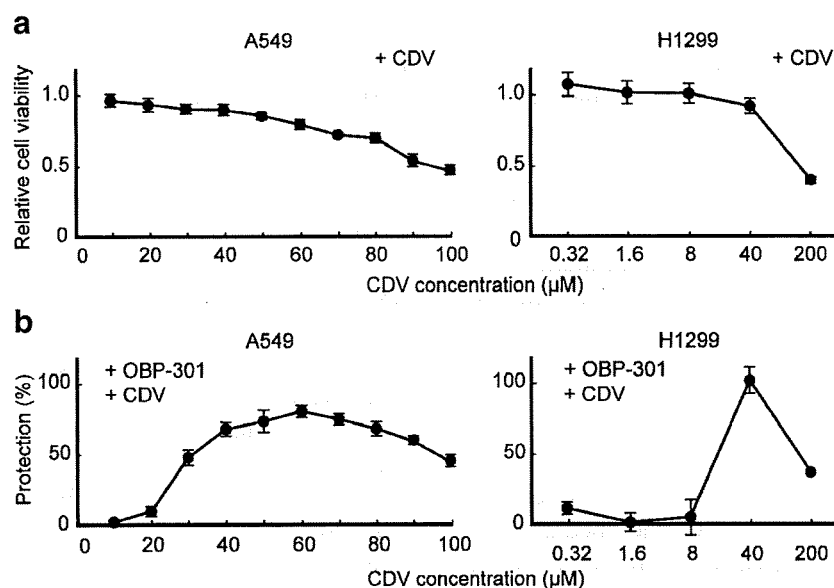


Fig. 2 Inhibition of cytopathic effects of OBP-301 by CDV in human lung cancer cell lines. (a) Cells were treated with CDV at the indicated concentrations and incubated for 7 days. The relative cell viability was evaluated by XTT assay. Data are mean±SD values. (b) Cells were

infected with OBP-301 (1 MOI in H1299 and 5 MOI in A549, PFU/cell), followed by the addition of CDV at the indicated concentrations. Protection was calculated as described in “Material and methods”. Data are mean±SD values

Discussion

OBP-301 has been developed as an oncolytic viral agent for the treatment of human cancer and is currently used in a phase-I clinical trial. Although replication of OBP-301 is limited in normal cells evaluated *in vitro* and *in vivo* mouse model, the effect of OBP-301 in human is still unknown. In the phase-II clinical trial of ONYX-015, an E1B-55 kDa-deleted adenovirus mutant, adenoviral viremia occurred even in the presence of neutralizing antibodies and antiviral cytokines [13]. Several antiviral drugs are used for other DNA viruses, e.g. aciclovir, a synthetic acyclic purine-nucleoside analogue, for Herpes simplex virus (HSV) [14], and ganciclovir (GCV) for Cytomegalovirus infections [15]. For AdV infections, it has been reported that CDV exhibits potent inhibitory effects against several adenoviral serotypes in cell culture models [10, 16]. We considered that CDV can be used as antiviral drug for OBP-301.

The purpose of using CDV clinically is to avoid toxic effects of OBP-301 in normal tissues, when viral replication becomes uncontrollable. However, it is difficult to examine the inhibitory effect of CDV on cytopathic effect of OBP-301 in normal cells, because OBP-301 replicates and lyses only in cancer cells [7–9]. Therefore, we used human cancer cell lines to assess the potential antiviral activity of CDV. We showed that the cytopathic effects of OBP-301 were efficiently suppressed by CDV treatment at concentrations that did not affect cell growth (Fig. 2). Despite the high susceptibility of H1299 cells to OBP-301 infection (Fig. 1), CDV inhibited the cytopathic effects of OBP-301, suggesting that CDV has potent antiviral activity against OBP-301. The 50% effective concentration of CDV in A549 cells was in agreement with the published data using human wt-Ad [17], indicating that the inhibitory activity against the cytopathic effect of OBP-301 was equivalent to that of wt-Ad.

The mechanism of the antiviral effect of CDV is that of inhibition of viral replication by targeting the viral DNA polymerase [18]. The anti-adenoviral effect of CDV is quantified by evaluating the viral progeny in adenovirus-infected cells using quantitative PCR analysis [16]. We demonstrated that the replication of OBP-301 was inhibited by CDV in a concentration-dependent manner (Fig. 3). In addition, the 50% effective concentration on viral DNA copy number was almost the same as the 50% effective concentration on cell death by OBP-301 infection, suggesting that CDV inhibited the cytopathic effect of OBP-301 by inhibiting the replication of OBP-301. Recently, antiviral effect of CDV against wt-Ad in immunosuppressed Syrian hamster model was reported [19]. The 50% inhibitory concentration of CDV on viral DNA copy number in OBP-301 was slightly higher than that of wt-Ad (Fig. 3). Differences at E1A region between OBP-301 and wt-Ad may

affect of CDV activity on viral replication. It has been reported that CDV-resistant human Ad mutants were isolated by continuous passage *in vitro* condition [20]. Quality assurance and quality control of the master virus bank have been intensively performed for OBP-301 used in the current clinical trials; emergence of CDV-resistant OBP-301 variant, however, should be considered and long-term susceptibility of CDV against OBP-301 will be studied in the future clinical trials.

In conclusion, our *in vitro* data indicate that CDV can effectively inhibit the oncolytic activity of OBP-301 by inhibiting the replication of OBP-301. CDV may be a potential antiviral agent for OBP-301 in clinical trial.

References

1. Kim D, Martuza RL, Zwiebel J (2001) Replication-selective virotherapy for cancer: biological principles, risk management and future directions. *Nat Med* 7:781–787. doi:10.1038/89901
2. Kim D (2000) Replication-selective oncolytic adenoviruses: virotherapy aimed at genetic targets in cancer. *Oncogene* 19:6660–6669. doi:10.1038/sj.onc.1204094
3. Chu RL, Post DE, Khuri FR, Van Meir EG (2004) Use of replicating oncolytic adenoviruses in combination therapy for cancer. *Clin Cancer Res* 10:5299–5312. doi:10.1158/1078-0432.CCR-0349-03
4. Davis JJ, Fang B (2005) Oncolytic virotherapy for cancer treatment: challenges and solutions. *J Gene Med* 7:1380–1389. doi:10.1002/jgm.800
5. Nakamura TM, Morfin GB, Chapman KB, Weinrich SL, Andrews WH, Lingner J et al (1997) Telomerase catalytic subunit homologs from fission yeast and human. *Science* 277:955–959. doi:10.1126/science.277.5328.955
6. Kim NW, Piatszek MA, Prowse KR, Harley CB, West MD, Ho PL et al (1994) Specific association of human telomerase activity with immortal cells and cancer. *Science* 266:2011–2015. doi:10.1126/science.7605428
7. Kawashima T, Kagawa S, Kobayashi N, Shirakiya Y, Umeoka T, Teraishi F et al (2004) Telomerase-specific replication-selective virotherapy for human cancer. *Clin Cancer Res* 10:285–292. doi:10.1158/1078-0432.CCR-1075-3
8. Taki M, Kagawa S, Nishizaki M, Mizuguchi H, Hayakawa T, Kyo S et al (2005) Enhanced oncolysis by a tropism-modified telomerase-specific replication-selective adenoviral agent OBP-405 (Telomelysin-RGD). *Oncogene* 24:3130–3140. doi:10.1038/sj.onc.1208460
9. Hashimoto Y, Watanabe Y, Shirakiya Y, Uno F, Kagawa S, Kawamura H et al (2008) Establishment of biological and pharmacokinetic assays of telomerase-specific replication-selective adenovirus. *Cancer Sci* 99:385–390. doi:10.1111/j.1349-7006.2007.00665.x
10. Gordon YJ, Romanowski E, Araullo-Cruz T, Seaberg L, Erzurum S, Tolman R et al (1991) Inhibitory effect of (S)-HPMPC, (S)-HPMPA, and 2'- β -nor-cyclic GMP on clinical ocular adenoviral isolates is serotype-dependent *in vitro*. *Antivir Res* 16:11–16. doi:10.1016/0166-3542(91)90054-U
11. De Clercq E (2003) Clinical potential of the acyclic nucleoside phosphonates cidofovir, adefovir, and tenofovir in treatment of DNA virus and retrovirus infections. *Clin Microbiol Rev* 16:569–596. doi:10.1128/CMR.16.4.569-596.2003

12. Kishimoto H, Kojima T, Watanabe Y, Kagawa S, Fujiwara T, Uno F et al (2006) *In vivo* imaging of lymph node metastasis with telomerase-specific replication-selective adenovirus. *Nat Med* 12:1213–1219. doi:10.1038/nm1404
13. Reid T, Galanis E, Abbruzzese J, Sze D, Wein LM, Andrews J et al (2002) Hepatic arterial infusion of a replication-selective oncolytic adenovirus (dl1520): phase II viral, immunologic, and clinical endpoints. *Cancer Res* 62:6070–6079
14. Whitley RJ, Roizman B (2001) Herpes simplex virus infection. *Lancet* 357:1513–1518. doi:10.1016/S0140-6736(00)04638-9
15. Biron KK (2006) Antiviral drugs for cytomegalovirus diseases. *Antivir Res* 71:154–163. doi:10.1016/j.antiviral.2006.05.002
16. Naesens L, Lenaerts L, Andrei G, Snoeck R, Van Beers D, Holy A et al (2005) Antiadenovirus activities of several classes of nucleoside and nucleotide analogues. *Antimicrob Agents Chemother* 49:1010–1016. doi:10.1128/AAC.49.3.1010-1016.2005
17. Morfin F, Dupuis-Girod S, Mundweiler S, Falcon D, Carrington D, Sedlacek P et al (2005) *In vitro* susceptibility of adenovirus to antiviral drugs is species-dependent. *Antivir Ther* 10:225–229
18. Kinchington PR, Araullo-Cruz T, Vergnes JP, Yates K, Gordon YJ (2002) Sequence changes in the human adenovirus type 5 DNA polymerase associated with resistance to the broad spectrum antiviral cidofovir. *Antivir Res* 56:73–84. doi:10.1016/S0166-3542(02)00098-0
19. Toth K, Spencer JF, Dhar D, Sagartz JE, Buller RM, Painter GR et al (2008) Hexadecyloxypropyl-cidofovir, CMX001, prevents adenovirus-induced mortality in a permissive, immunosuppressed animal model. *Proc Natl Acad Sci U S A* 105:7293–7297. doi:10.1073/pnas.0800200105
20. Gordon YJ, Araullo-Cruz TP, Johnson YF, Romanowski EG, Kinchington PR (1996) Isolation of human adenovirus type 5 variants resistant to the antiviral cidofovir. *Invest Ophthalmol Vis Sci* 37:2774–2778

Preclinical evaluation of synergistic effect of telomerase-specific oncolytic virotherapy and gemcitabine for human lung cancer

Dong Liu,^{1,3} Toru Kojima,^{1,2} Masaaki Ouchi,⁴ Shinji Kuroda,^{1,2} Yuichi Watanabe,^{2,4} Yuuri Hashimoto,^{2,4} Hideki Onimatsu,⁴ Yasuo Urata,⁴ and Toshiyoshi Fujiwara^{1,2}

¹Center for Gene and Cell Therapy, Okayama University Hospital; ²Division of Surgical Oncology, Department of Surgery, Okayama University Graduate School of Medicine, Dentistry and Pharmaceutical Sciences, Okayama, Japan; ³Research Center of Lung Cancer, Shanghai Pulmonary Hospital, The Tongji University, Shanghai, China; and ⁴Oncolys BioPharma, Inc., Tokyo, Japan

Abstract

A phase I dose-escalation study of telomerase-specific oncolytic adenovirus, OBP-301 (Telomelysin), is now under way in the United States to assess feasibility and to characterize its pharmacokinetics in patients with advanced solid tumors. The present preclinical study investigates whether OBP-301 and a chemotherapeutic agent that is commonly used for lung cancer treatment, gemcitabine, are able to enhance antitumor effects *in vitro* and *in vivo*. The antitumor effects of OBP-301 infection and gemcitabine were evaluated by 2,3-bis[2-methoxy-4-nitro-5-sulfophenyl]-2H-tetrazolium-5-carboxanilide inner salt assay. *In vivo* antitumor effects of intratumoral injection of OBP-301 in combination with systemic administration of gemcitabine were assessed on *nu/nu* mice s.c. xenografted with human lung tumors. OBP-301 infection combined with gemcitabine resulted in very potent synergistic cytotoxicity in human lung cancer cells. The three human lung cancer cell lines treated with OBP-301 for 24 hours tended to accumulate in S phase compared with controls. The proportion of cells in S phase increased from 43.85% to 56.41% in H460 cells, from 46.72% to 67.09% in H322 cells, and from 38.22% to 57.67% in H358 cells. Intratumoral injection of OBP-301 combined

with systemic administration of gemcitabine showed therapeutic synergism in human lung tumor xenografts. Our data suggest that the combination of OBP-301 and gemcitabine enhances the antitumor effects against human lung cancer. We also found that the synergistic mechanism may be due to OBP-301-mediated cell cycle accumulation in S phase. These results have important implications for the treatment of human lung cancer. [Mol Cancer Ther 2009;8(4):980–7]

Introduction

Lung cancer is the most common cause of cancer-related mortality. In current clinical practice, chemotherapy is used in combination with radiotherapy as an adjuvant or neoadjuvant therapy. Moreover, combination chemotherapy is regarded as the standard care in the treatment of unresectable locally advanced (stage IIIB), metastatic (stage IV), or recurrent disease. Although there have been major improvements over recent decades in surgical techniques and the role of chemotherapy-radiotherapy in the treatment of non-small cell lung cancer, the long-term outlook for such patients has not changed significantly. The median survival for patients with advanced-stage non-small cell lung cancer treated with platinum-based chemotherapy is a disappointing 8 to 10 months (1). Clearly, new therapies are needed that are capable of treating such advanced cancers in addition to preventing their formation.

One type of cancer therapy that has been extensively investigated is virotherapy, which uses oncolytic viruses engineered to selectively replicate within tumor cells, killing them. We previously developed an adenovirus vector that drives the *E1A* and *E1B* genes under the hTERT promoter, designated OBP-301 (Telomelysin), and showed its selective replication, as well as its profound cytotoxic activity, in a variety of human cancer cells (2–5). Although the development of OBP-301 as a monotherapy is currently under way clinically based on the promising preclinical results, multimodal strategies to enhance antitumor efficacy *in vivo* are essential for successful clinical outcome. In fact, most clinical trials for oncolytic viruses have been conducted in combination with chemotherapy or radiotherapy (6).

Gemcitabine (2,2-difluorodeoxycytidine) is a third-generation agent that has been developed in the past decades. Gemcitabine is a deoxycytidine analogue that has shown efficacy as a treatment for many solid tumors and is now extensively used in the treatment of patients with various tumor types (7, 8), but inherent and acquired resistance has resulted in low response rates. In the present study, we hypothesized that combination of oncolytic adenoviral agents (with novel mechanisms of action) with

Received 9/19/08; revised 12/15/08; accepted 1/20/09.

Grant support: Ministry of Education, Science, and Culture, Japan (T. Fujiwara); Ministry of Health and Welfare, Japan (T. Fujiwara); and Japan China Medical Association (D. Liu).

The costs of publication of this article were defrayed in part by the payment of page charges. This article must therefore be hereby marked *advertisement* in accordance with 18 U.S.C. Section 1734 solely to indicate this fact.

Requests for reprints: Toshiyoshi Fujiwara, Center for Gene and Cell Therapy, Okayama University Hospital, 2-5-1 Shikata-cho, Okayama 700-8558, Japan. Phone: 81-86-235-7997; Fax: 81-86-235-7884. E-mail: toshi_f@md.okayama-u.ac.jp

Copyright © 2009 American Association for Cancer Research.

doi:10.1158/1535-7163.MCT-08-0901

chemotherapeutic agents could improve the antitumor effects and minimize the toxic side effects of the latter by reducing the concentrations of anticancer drugs. To test our hypothesis, we examined the therapeutic effects of OBP-301 combined with gemcitabine both *in vitro* and *in vivo*. The results showed that combination therapy with OBP-301 and gemcitabine produced therapeutic benefits over either individual modality.

Materials and Methods

Cell Lines and Cell Cultures

The human large cell lung cancer cell line H460, the bronchioloalveolar carcinoma cell line H322, and the bronchioloalveolar carcinoma cell line H358 were propagated in monolayer culture in RPMI 1640 supplemented with 10% FCS.

Chemotherapeutic Agents and Viruses

Gemcitabine (Gemzar) was obtained from Eli Lilly Co. Stock solution was prepared in 0.9% NaCl and the agent was further diluted in growth medium immediately before use. OBP-301 is a telomerase-specific replication-competent adenovirus variant, in which the hTERT promoter element drives the expression of *E1A* and *E1B* linked with internal ribosomal entry site. The virus was purified by ultracentrifugation in cesium chloride step gradients and titer was determined by plaque assay in 293 cells, as described previously (2–5).

Cell Viability Assay

2,3-Bis[2-methoxy-4-nitro-5-sulfophenyl]-2H-tetrazolium-5-carboxanilide inner salt (XTT) assay was done to assess the viability of tumor cells. H460, H322, and H358 cells at 1,000 per well were seeded onto 96-well plates at 18 to 20 h before viral infection. Cells were then infected with OBP-301 at low to high concentrations and were treated with fresh medium containing gemcitabine at various concentrations at 24 h after OBP-301 infection. Cell viability was determined at 4 d after treatment with OBP-301 and gemcitabine by using a Cell Proliferation Kit II (Roche Molecular Biochemicals) according to the protocol provided by the manufacturer.

In vitro Replication Assay

H460, H322, and H358 cells were seeded in six-well plates at 10^5 per well at 12 h before infection. Cells were infected with OBP-301 at a multiplicity of infection (MOI) of 10, 25, and 20 plaque-forming units (pfu)/cell, respectively, and fresh medium containing gemcitabine at 70 nmol/L for H460 cells, 100 nmol/L for H322 cells, and 3 nmol/L for H358 cells was then added at 24 h after infection. Cells were incubated at 37°C, trypsinized, and harvested for intracellular replication analysis at 2, 24, 48, 72, 96, and 108 h after OBP-301 infection. DNA purification was done using QIAmp DNA Mini kit (Qiagen, Inc.). The *E1A* DNA copy number was determined by quantitative real-time PCR using a LightCycler instrument and LightCycler-DNA Master SYBR Green I (Roche Diagnostics).

Assessment of *E1A* Expression by Western Blotting

H460, H322, and H358 cells infected with OBP-301 at an MOI of 10, 25, and 20, respectively, were collected at 5 d after infection, lysed in lysis buffer [10 mmol/L Tris-HCl (pH 7.5), 400 mmol/L NaCl, 1 mmol/L DTT, 5 mmol/L NaF, 1 mmol/L EDTA, 0.5% Na_3VO_4 , 10% glycerol, 0.5% NP40, 0.1 mmol/L phenylmethylsulfonyl fluoride, 1 mg/mL leupeptin, 1 mg/mL aprotinin] for 30 min on ice, and centrifuged at 15,000 rpm for 30 min. Protein concentration was measured by means of the Bradford assay. Equal amounts of protein-containing sample buffer [62.5 mmol/L Tris-HCl (pH 6.8), 2% SDS, 10% glycerol, 5% β -mercaptoethanol] were boiled for 5 min and electrophoresed under reducing conditions on 12% (w/v) polyacrylamide gels. Proteins were electrophoretically transferred to Hybond polyvinylidene difluoride transfer membranes (Amersham) and incubated with primary antibody against *E1A* (BD Pharmingen) or rabbit anti-human β -actin monoclonal antibody (Sigma-Aldrich) followed by peroxidase-linked secondary antibody. An enhanced chemiluminescence Western system (Amersham) was used to detect secondary probes.

Cell Cycle Analysis

H460, H322, and H358 cells were infected with OBP-301 at 40, 100, and 80 MOI, respectively, for 24 h. The cells were then harvested and suspended in 1.5 mL PBS before fixing with ice-cold 70% ethanol for 30 min. Fixed samples were centrifuged for 5 min, and cell pellets were resuspended in 700 μ L PBS containing RNase (0.25 mg/mL) followed by incubation for 30 min at 37°C. The volume was increased to 1 mL with PBS containing 1% bovine serum albumin and propidium iodide (50 μ g/mL) and the suspensions were incubated at 4°C for 30 min. Stained cells were analyzed by FACScan (Becton Dickinson) and by WinMDI v2.8 software (Scripps Institute).

Assessment of Cell Cycle Regulator Protein Expression by Western Blotting

H460, H322, and H358 cells were infected with OBP-301 at 40, 100, and 80 MOI, respectively, before harvesting 24 h later. Collected cells were analyzed for expression of *E2F1*, *p53*, and *E1A* and phosphorylation of Akt. Primary antibodies were purchased from Santa Cruz Biotechnology (*E2F1*), Calbiochem Co. (*p53*), and Sigma Co. (β -actin). Protein expression was quantified by densitometric scanning using NIH Image software.

In vivo Human Tumor Model

H358 cells (5×10^6 per mouse) were injected s.c. into the backs of 5- to 6-wk-old female BALB/c *nu/nu* mice and were permitted to grow to 5 to 10 mm in diameter. At that time, mice were randomly assigned into four groups: mock, OBP-301, gemcitabine, and OBP-301 plus gemcitabine. Next, 50 μ L of solution containing OBP-301 at a dose of 1×10^7 pfu/body or PBS were injected into the tumors. Simultaneously, each mouse in the combination group and gemcitabine group received an i.p. injection of 100 μ L gemcitabine at a dose of 70 mg/kg every 3 d for three cycles starting at day 0. The perpendicular

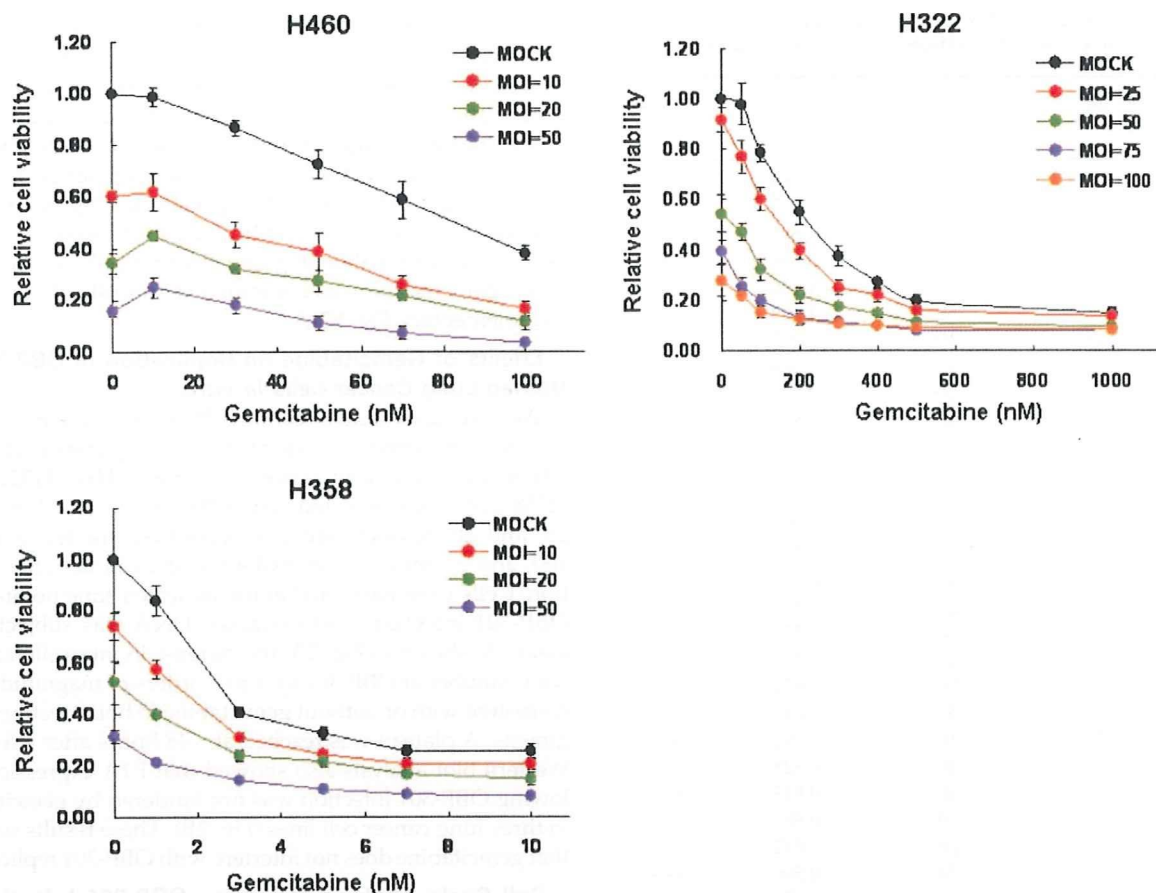


Figure 1. Combination efficiency of OBP-301 and gemcitabine on human lung cancer cell lines. H460, H322, and H358 cells were infected with OBP-301 at the indicated MOIs and then exposed to gemcitabine at the indicated concentrations at 24 h after infection. Cell viability was assessed by XTT assay at 5 d after OBP-301 infection. Bars, SD.

diameter of each tumor was measured every 3 d, and tumor volume was calculated using the following formula: tumor volume (mm^3) = $a \times b^2 \times 0.5$, where a is the longest diameter, b is the shortest diameter, and 0.5 is a constant used to calculate the volume of an ellipsoid. The experimental protocol was approved by the Ethics Review Committee for Animal Experimentation of Okayama University.

Statistical Analysis

Determinations of significant differences in mean tumor size among groups were assessed by calculating the value of Student's t using the original data analysis.

Results

Antitumor Efficacy of OBP-301 Combined with Gemcitabine in Human Lung Cancer Cell Lines *In vitro*

Before we tested the combination efficacy, sensitivity to gemcitabine and OBP-301 was evaluated in a variety of human lung cancer cell lines by the XTT method, and we selected three cell lines, H460, H322, and H358, for further experiments. From the XTT experiments with gemcitabine

alone or OBP-301 alone (Supplementary Fig. S1),⁵ the optimal concentrations of gemcitabine and OBP-301 were determined for each cell line. To examine the potential interaction between gemcitabine and OBP-301 *in vitro*, cell viability with six to eight different doses of OBP-301 and four to five doses of gemcitabine was then assessed by XTT assay at 5 days after treatment. Representative dose-response curves are shown in Fig. 1. All cell lines treated with OBP-301 and gemcitabine showed reduced viability when compared with cells treated with single agents.

We then used software to analyze the combination efficiency in these three cell lines (Table 1). In H358 cells, OBP-301 and gemcitabine were apparently synergistic at most doses, whereas the effect of the combination was mostly additive in H322 cells. In H460 cells, the effect was additive when the concentration of gemcitabine was 50 nmol/L; with the increasing of the concentration, however, a clear synergistic effect was seen. When the concentration was 100 nmol/L, synergism was apparent. These

⁵ Supplementary data for this article are available at Molecular Cancer Therapeutics Online (<http://mct.aacrjournals.org/>).

Table 1. Combination index value analysis by CalcuSyn software (version 2) of combination efficiency in human lung cancer cells

Cells	Gemcitabine (nmol/L)	OBP-301 (MOI)	Combination index	Synergy
H460	10	10	1.261	--
		20	1.405	--
		50	1.688	--
	30	10	0.996	±
		20	1.106	-
		50	1.349	--
	50	10	1.037	±
		20	1.104	-
		50	0.998	±
	70	10	0.87	+
		20	1.037	±
		50	0.793	++
	100	10	0.793	++
		20	0.785	++
		50	0.531	+++
H358	1	10	0.952	±
		20	0.812	++
		50	0.772	++
	3	10	0.713	++
		20	0.674	+++
		50	0.641	+++
	5	10	0.792	++
		20	0.828	++
		50	0.613	+++
	7	10	0.88	+
		20	0.812	++
		50	0.596	+++
	10	10	1.178	-
		20	0.948	±
		50	0.693	+++
H322	50	25	1.028	±
		50	0.941	±
		75	0.874	++
	100	100	1.033	±
		25	0.953	±
		50	0.842	++
	200	75	0.848	++
		100	0.938	±
		25	0.944	±
	300	50	0.856	+
		75	0.82	++
		100	0.979	±
	400	25	0.912	±
		50	1.024	±
		75	0.887	+
500	100	0.887	+	
	25	1.005	±	
	50	0.975	±	
	75	1.093	±	
	100	0.938	±	
	25	0.977	±	
	50	0.97	±	
	75	0.946	±	
	100	1.154	-	

NOTE: Range of combination index symbol descriptions: 0.3 to 0.7, +++, synergism; 0.7 to 0.85, ++, moderate synergism; 0.85 to 0.90, +, slight synergism; 0.90 to 1.10, ±, additive; 1.10 to 1.20, -, slight antagonism; 1.20 to 1.45, --, moderate antagonism.

results suggest that combination treatment with OBP-301 plus gemcitabine was effective in all cell lines tested.

We also assessed the morphologic changes in cells treated with either the combination modality or single agents. Phase-contrast images at 96 hours after OBP-301 infection showed the growth of cells to subconfluence without morphologic changes in the presence of gemcitabine, whereas a rapid loss of viability due to massive cell death, as evidenced by ballooning and floating cells, was evident when gemcitabine was combined with OBP-301 infection (Supplementary Fig. S2).⁵

Effects of Gemcitabine on Replication of OBP-301 in Human Lung Cancer Cells *In vitro*

We used quantitative real-time PCR and Western blotting to assess the effects of gemcitabine on replication of OBP-301 in the three lung cancer cell lines. H460, H322, and H358 cells were infected with OBP-301 at an MOI of 10, 25, and 20, respectively, and were then treated with 70, 100, and 3 nmol/L of gemcitabine at 24 hours after infection. Cells were harvested at the indicated time points after OBP-301 infection, and extracted DNA was subjected to assay. As shown in Fig. 2A, the increase in intracellular viral copy number of OBP-301 by 4 to 5 orders of magnitude was consistent with or without gemcitabine in both treatment regimens. A plateau was reached at ~48 hours after infection. Western blot analysis also showed that E1A expression following OBP-301 infection was not hindered by gemcitabine in three lung cancer cell lines (Fig. 2B). These results suggest that gemcitabine does not interfere with OBP-301 replication.

Cell Cycle Analysis following OBP-301 Infection in Human Lung Cancer Cells

To further explore the "greater than additive response" observed when cells were infected with OBP-301 followed by gemcitabine treatment, we carried out cell cycle analysis of these cells after OBP-301 infection by flow cytometric analysis of propidium iodide-stained cells, a measure of DNA content. As shown in Fig. 3A, the cell cycle distribution apparently changed compared with mock-infected cells at 24 hours after OBP-301 infection in all cell lines tested, although there was no increase in the sub-G₀-G₁ population indicating apoptotic cell death. The number of cells in S phase increased from 43.85% to 56.41% in H460 cells, from 46.72% to 67.09% in H322 cells, and from 38.22% to 57.67% in H358 cells (Table 2). These results suggest that OBP-301 is able to accumulate infected cells in S phase, which may render cells more sensitive to gemcitabine.

Changes in Cell Cycle Regulator Protein Expression following OBP-301 Infection

To clarify the mechanisms of cell cycle regulation by OBP-301, we analyzed the expression of proteins that have a crucial role in the cell cycle. H460, H322, and H358 cells were infected with OBP-301 at an MOI of 40, 100, and 80, and Western blot analysis was then done 24 hours later. As shown in Fig. 3B, expression levels of E2F1, as well as phosphorylated Akt, greatly increased after OBP-301 infection compared with the mock-infected controls in all three cell lines. p53 protein expression was not detectable in H460

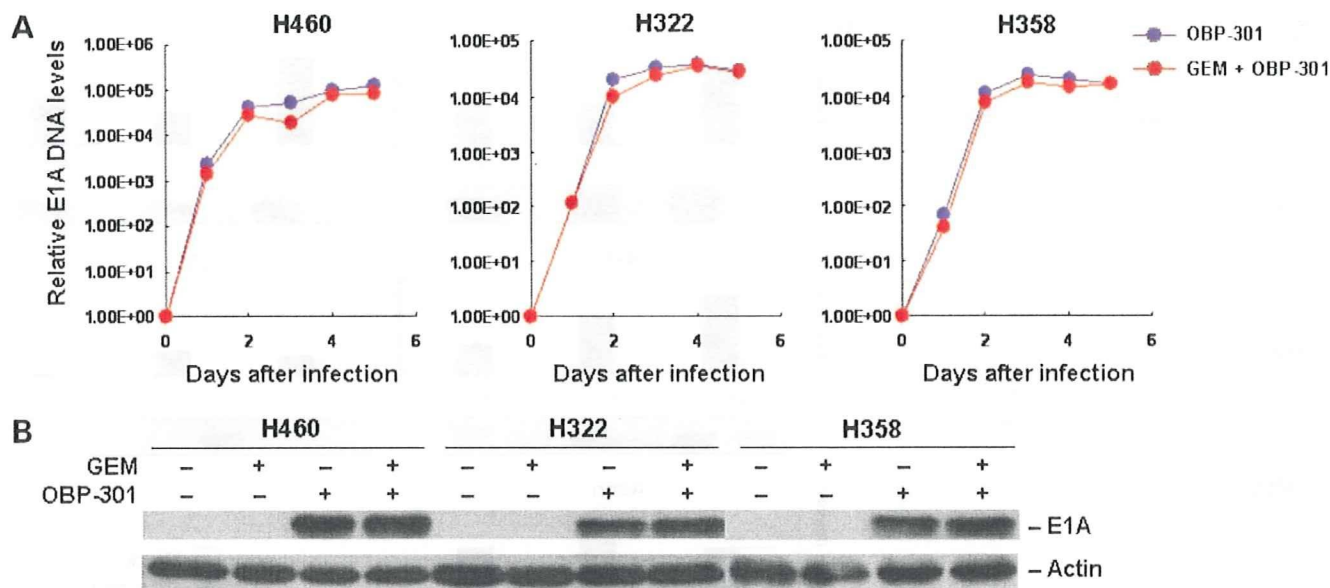


Figure 2. Assessment of viral DNA replication in human lung cancer cells. **A**, H460, H322, and H358 cells were infected with OBP-301 at an MOI of 10, 25, and 20, respectively, for 2 h as a baseline for virus DNA levels. Following the removal of virus inocula at 24 h after the infection, H460, H322, and H358 cells were further incubated with 70, 100, and 3 nmol/L of gemcitabine (*GEM*), respectively, for the indicated periods of time. Cells were then subjected to quantitative real-time PCR assay. Viral E1A copy number was defined as the fold increase for each sample relative to that at 2 h (2 h = 1). **B**, Western blot analysis of E1A expression in human lung cancer cells. Cells were treated with OBP-301, gemcitabine, or a combination of both, as described above, and then subjected to assay at 4 d after infection.

expressing the wild-type *p53* gene and *p53*-null H358 cells, whereas OBP-301 infection down-regulated mutant *p53* expression in H322 cells.

Antitumor Effects of OBP-301 plus Gemcitabine in Human Lung Cancer Xenografts

Finally, we assessed the therapeutic efficacy of OBP-301 in combination with gemcitabine against H358 human lung cancer cells *in vivo*. H358 cells were implanted as xenografts into the hind flanks of *nu/nu* mice. Mice bearing palpable H358 tumors measuring 5 to 7 mm in diameter received simultaneous treatment of intratumoral injection of either 10^7 pfu OBP-301 or PBS plus *i.p.* administration of either 70 mg/kg gemcitabine or PBS every 3 days for three cycles starting at day 0. As shown in Fig. 4, administration of gemcitabine resulted in significant tumor growth suppression compared with mock-treated tumors for 34 days after initiation of treatment ($P < 0.05$); the combination of OBP-301 plus gemcitabine, however, produced a more profound and significant inhibition of tumor growth compared with mice treated with gemcitabine alone for at least 45 days ($P < 0.05$). The addition of OBP-301 clearly prolonged the antitumor effects of gemcitabine. Intratumoral injection of a replication-deficient adenovirus with or without systemic administration of gemcitabine had no apparent effect on the growth of H358 tumors (data not shown).

Discussion

Replication-competent oncolytic adenoviruses are promising as a novel anticancer therapy (9). In our laboratory, a tumor-specific replication-selective adenovirus, designated

Telomelysin or OBP-301, is effective against human cancers (2–5). This virus was genetically designed to replicate under the control of hTERT promoter specifically in tumor cells, causing specific oncolysis. Despite the encouraging outcomes in animal experiments, combination chemotherapy and virotherapy are recommended in clinical treatment, as tumor progression is very rapid in most patients. In the current study, we explored the combination effects of OBP-301 and gemcitabine in human lung cancer cells *in vitro* and *in vivo*.

Adenovirus therapy combined with gemcitabine has been reported in the treatment of pancreatic cancer. Halloran et al. (9) reported that incubation of Panc-1 cells with either 5-fluorouracil or gemcitabine followed by adenovirus-mediated overexpression of $p16^{\text{INK4A}}$ resulted in a substantial reduction in cell viability under conditions where the drugs alone had minimal cytotoxicity. Although most studies reporting the combination effects of gemcitabine and adenoviral agents for pancreatic tumor used therapeutic genes critical for tumor growth inhibition, OBP-301 itself is an effective oncolytic virus and leads to infected cell destruction. Moreover, it has been reported that the type 5 adenoviral E1A sensitizes hepatocellular carcinoma cells to gemcitabine (10). These observations support the notion that oncolytic adenoviruses combined with gemcitabine are a rational modality for the treatment of human cancer.

The antitumor efficacy of OBP-301 was found to be enhanced when combined with gemcitabine in human lung cancer cells *in vitro* (Fig. 1; Table 1). Synergistic interaction was apparent in H460 and H358 cells; the combination

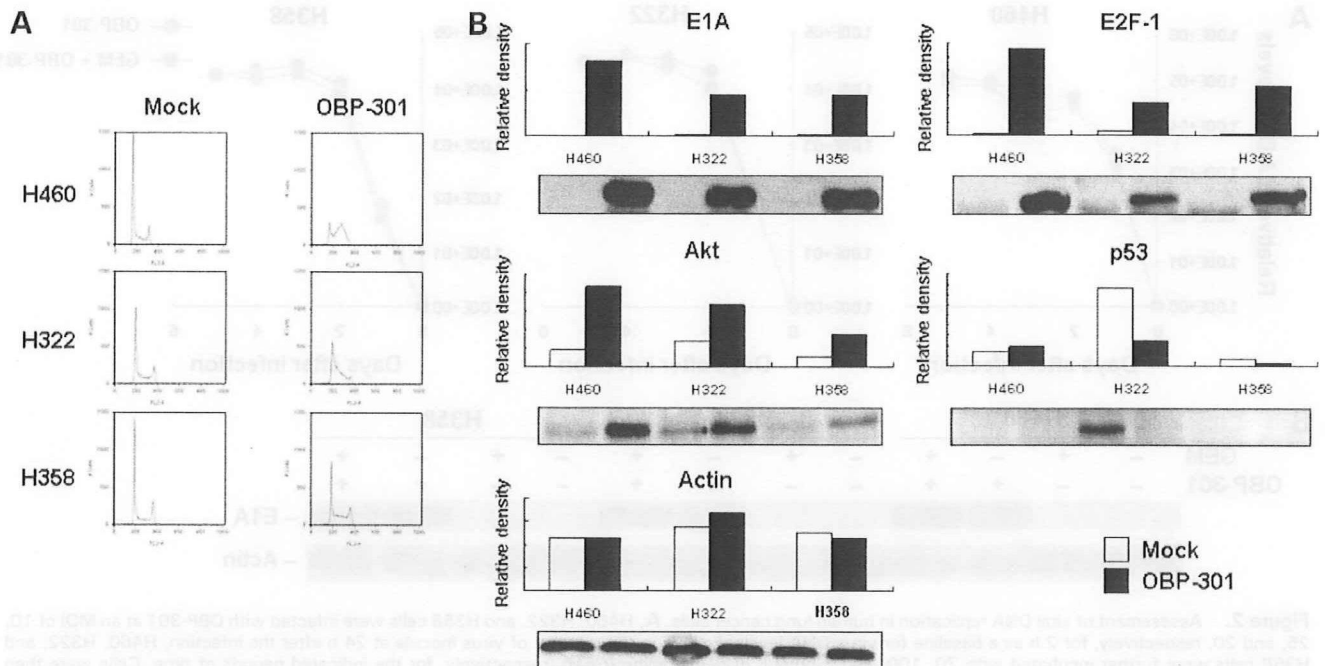


Figure 3. Cell cycle analysis and Western blotting of cell cycle regulator protein following OBP-301 infection in human lung cancer cells. **A**, H460, H322, and H358 cells were infected with OBP-301 at an MOI of 40, 100, and 80 MOI, respectively. DNA content was determined by propidium iodide staining and flow cytometric analysis at 24 h after OBP-301 infection. **B**, H460, H322, and H358 cells were either mock infected or infected with OBP-301 at an MOI of 40, 100, and 80 MOI, respectively. Following the removal of virus inocula, cells were collected at 24 h after infection and subjected to analysis. Equivalent amounts of protein obtained from whole-cell lysates were loaded into each lane, probed with primary antibodies, and then visualized using an enhanced chemiluminescence detection system. Equal loading of samples was confirmed by reprobing with antiactin antiserum. Protein expression was quantified by densitometric scanning using NIH Image software.

effect, however, was additive in H322 cells, suggesting that the effect of the combination is dependent on cell type. We also confirmed that this synergistic effect could be observed in human pancreatic cancer cells (Supplementary Fig. S3).⁵ Gemcitabine is a deoxycytidine analogue and the incorporation of gemcitabine triphosphate into DNA causes chain termination, which is the major mechanism underlying the cytotoxicity of gemcitabine (11). Although there was concern over whether gemcitabine would interrupt the viral replication of OBP-301, quantitative real-time PCR analysis showed that intracellular replication of OBP-301 was not affected by gemcitabine (Fig. 2). The cytotoxic mechanisms of OBP-301 are distinct from those of gemcitabine, and therefore, combination effects could be observed provided that gemcitabine does not inhibit viral replication.

To clarify the mechanisms of the greater than additive response, cell cycle analysis was done following OBP-301 infection. Cells treated with OBP-301 tended to accumulate in the S phase at 24 hours after infection (Fig. 3A; Table 2). It has been reported that many DNA viruses can drive quiescent cells through G₁ into S phase by the expression of viral proteins (12–14). During the early phase of the adenovirus infection, the host cell is transformed into an efficient producer of the viral genome. The first gene that is transcribed in the viral genome is *E1A*, which can bind to numerous cellular proteins and acts as a multifunctional

protein. Our data showed that OBP-301 infection increases the phosphorylation of Akt, as well as E2F1 expression, in all three human lung cancer cell lines (Fig. 3B). These effects are thought to be due to adenoviral E1A protein expression, as the dl312 adenovirus lacking the E1 genes did not phosphorylate Akt (data not shown).

Direct evidence of cell cycle promotion by Akt was seen when coexpression of Akt rescued cells from PTEN-induced cell cycle arrest (15). Retinoblastoma (Rb) protein restrains proliferation, in part, by modulating the activity of E2F

Table 2. Cell cycle analysis after OBP-301 infection in human lung cancer cells

Cell lines	Treatment	Cell cycle		
		G ₁ (%)	S (%)	G ₂ (%)
H460	Mock	43.54	43.85	8.61
	OBP-301	10.91	56.41	32.54
H322	Mock	40	46.72	10.85
	OBP-301	27.49	67.09	3.23
H358	Mock	45.89	38.22	14.29
	OBP-301	28.93	57.67	11.45

NOTE: H460, H322, and H358 cell lines were treated with OBP-301 at 40, 100, and 80 MOI, respectively. Cells were then subjected to cell cycle analysis at 24 h after treatment by the fluorescence-activated cell sorting method. The percentages of cells in the G₁, S, and G₂ phases are shown.

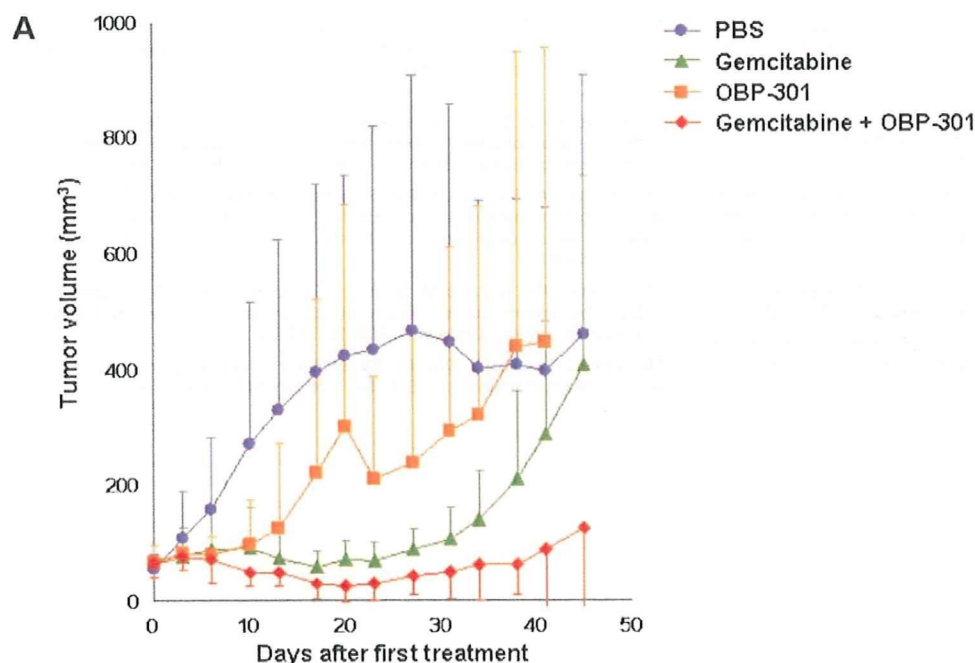


Figure 4. Antitumor effects of intratumorally injected OBP-301 and i.p. administered gemcitabine against established back H358 xenograft tumors in *nu/nu* mice. **A**, H358 tumor cells (5×10^6 /each) were s.c. injected into the right flanks of mice. OBP-301 (1×10^8 pfu/body) and gemcitabine (70 mg/kg) were administered intratumorally and i.p., respectively, for three cycles every 3 d. PBS was used as the control. Eight mice were used for each group. Tumor growth is expressed as mean volume \pm SE. **B**, statistical analysis was done using Student's *t* test for differences among indicated groups. Statistical significance (red number) was defined as $P < 0.05$.

	Day 23	Day 27	Day 31	Day 34	Day 38	Day 41	Day 45
PBS vs OBP-301	0.116	0.172	0.354	0.588	0.870	0.788	0.774
PBS vs Gemcitabine (GEM)	0.015	0.025	0.020	0.021	0.073	0.336	0.773
PBS vs GEM + OBP-301	0.009	0.014	0.014	0.005	0.004	0.008	0.051
OBP-301 vs GEM	0.034	0.068	0.101	0.155	0.198	0.377	0.594
OBP-301 vs OBP-301 + GEM	0.011	0.024	0.021	0.050	0.044	0.054	0.080
GEM vs OBP-301 + GEM	0.013	0.007	0.022	0.029	0.015	0.012	0.033

transcription factors. In quiescent cells, Rb associates with several E2Fs, resulting in the repression of proliferation-associated genes. As cells progress into the cell cycle, cyclin-dependent kinases phosphorylate Rb, freeing E2F and allowing it to directly transactivate genes required for S-phase entry (16). In fact, replication-deficient adenovirus-mediated *E2F1* gene transfer into human cancer cells resulted in accumulation of an S-phase cell population (Supplementary Fig. S4).⁵ Thus, OBP-301 infection expressed E1A protein, which in turn up-regulated the expression of phosphorylated Akt and E2F1, leading to cell cycle promotion and S-phase entry presumably by the deactivation of Rb. Indeed, we confirmed that OBP-301 infection decreased Rb protein expression in H460 cells (data not shown). The accumulation of the tumor cells in S phase increases the cytotoxicity of gemcitabine, which kills cells in S phase.

In summary, our data show that telomerase-specific oncolytic adenovirus infection increases the sensitivity of human lung cancer cells to gemcitabine due to S-phase accumulation. The combination of OBP-301 and gemcitabine efficiently inhibits human cancer cell growth both *in vitro* and *in vivo*, an outcome that has important implications for tumor-specific oncolytic chemovirotherapies for human lung cancer.

Disclosure of Potential Conflicts of Interest

M. Ouchi, H. Onimatsu, and Y. Urata: employees of Oncolys BioPharma, Inc. T. Fujiwara: consultant for Oncolys BioPharma, Inc. No other potential conflicts of interest were disclosed.

Acknowledgments

We thank Daiju Ichimaru and Hitoshi Kawamura for their helpful discussions and Tomoko Sueishi for her excellent technical support.

References

- Gkiozos I, Charpidou A, Syrigos K. Developments in the treatment of non-small cell lung cancer. *Anticancer Res* 2007;27:2823–7.
- Kawashima T, Kagawa S, Kobayashi N, et al. Telomerase-specific replication-selective virotherapy for human cancer. *Clin Cancer Res* 2004;10:285–92.
- Taki M, Kagawa S, Nishizaki M, et al. Enhanced oncolysis by a tropism-modified telomerase-specific replication-selective adenoviral agent OBP-405 ('Telomelysin-RGD'). *Oncogene* 2005;24:3130–40.
- Hashimoto Y, Watanabe Y, Shirakiya Y, et al. Establishment of biological and pharmacokinetic assays of telomerase-specific replication-selective adenovirus. *Cancer Sci* 2008;99:385–90.
- Endo Y, Sakai R, Ouchi M, et al. Virus-mediated oncolysis induces danger signal and stimulates cytotoxic T-lymphocyte activity via proteasome activator upregulation. *Oncogene* 2008;27:2375–81.
- Khuri FR, Nemunaitis J, Ganly I, et al. A controlled trial of intratumoral ONYX-015, a selectively-replicating adenovirus, in combination with cisplatin and 5-fluorouracil in patients with recurrent head and neck cancer. *Nat Med* 2000;6:879–85.